Time-varying n-threshold Gerber correlation and application in portfolio optimization

by

Gyu Hwan Park

A thesis submitted in partial fulfillment for the
degree of Master of Data Science

at the
THE UNIVERSITY OF MELBOURNE

October 2023

THE UNIVERSITY OF MELBOURNE

Abstract

Master of Data Science

by Gyu Hwan Park

This master's thesis extends the Gerber correlation statistic (Gerber et al., 2022) and investigates its performance in Mean-Variance Portfolio Optimization settings (Markowitz, 1952). We extend the original Gerber correlation statistic that only uses a single threshold level and define the notion of concordance and discordance of random variables that allow for an arbitrary number of n thresholds. Empirical study shows that such extension leads to more robust portfolio performance with improved annualized portfolio returns and Sharpe Ratio in most scenarios, especially in volatile regimes like during COVID. Moreover, we develop the Exponentially Weighted Moving Average Gerber correlation statistic that allows for the estimation of time-varying co-movement structure between asset returns under the structure of Gerber correlation. Empirical study shows that using such covariance measure in portfolio optimization can achieve enhanced portfolio performance, as it can automatically adapt to ever-changing market situations.

Declaration of Authorship

I certify that this report does not incorporate without acknowledgement any material previously submitted for a degree or diploma in any university; and that to the best of my knowledge and belief it does not contain any material previously published or written by another person where due reference is not made in the text. The report is 11000 words in length (excluding text in images, tables, bibliographies and appendices).

Signed:

Date: 23/10/2023

Acknowledgements

I would like to express my heartfelt gratitude to Dr. Pavel Krupskiy, my dedicated and insightful supervisor, for his expertise and unwavering guidance throughout the entire journey of my master's thesis. Dr. Krupskiy's mentorship has been instrumental in shaping the research and the quality of this thesis.

I am deeply indebted to my family for their unwavering love, encouragement, and belief in me. Their constant support and understanding have been my pillars of strength, and I am immensely thankful for the sacrifices they made to make this academic endeavor possible.

I would also like to extend my gratitude to my friends who have been a source of motivation, inspiration, and camaraderie. Your encouragement and willingness to lend a listening ear during both challenging and joyous times have been invaluable.

To all those who have contributed to my academic and personal growth, whether through encouragement, constructive feedback, or simply being there when I needed it most, I extend my heartfelt appreciation. This thesis would not have been possible without your collective support.

Thank you.

Contents

List of Figures

List of Tables

Abbreviations

AR	**A**uto **R**egressive
ARMA	**A**uto **R**egressive Moving **A**verage
EWMA	**E**xpoentially **W**eighted Moving **A**verage
GARCH	**G**eneralized **A**uto **R**egressive **C**onditional **H**eteroscedasticity
LSTM	**L**ong **S**hort-**T**erm Memory
MVP	Mean-**V**ariance **P**ortfolio
PD	**P**ositive **D**efinite
PSD	**P**ositive **S**emi-**D**efinite
VaR	**V**alue **at** **R**isk

Symbols

Symbol	Meaning
a	a non-bold, lower-case letter denotes a scalar constant.
$\boldsymbol{a}$	a bold, lower-case letter denotes a vector with entries $a_1, \ldots, a_K$.
$\boldsymbol{A}$	a bold, upper-case letter denotes a matrix.
^{T}	the transpose of a vector or matrix.
$\sim N_K(\boldsymbol{\mu}, \boldsymbol{\Sigma})$	denotes that a K-dimensional random variable is multi-variate normally distributed with mean $\boldsymbol{\mu}$ and covariance matrix $\boldsymbol{\Sigma}$.
$\mathrm{diag}(\boldsymbol{a})$	a diagonal matrix with elements $a_1, \ldots, a_K$ along the diagonal.
$\{a_i\}_{i=1}^n$	a sequence of a_i values where $i = 1, \ldots, n$.
$[a_{ij}]_{i=1, j=1}^{K, \ K}$	a $K \times K$ matrix with a_{ij} in the (i, j)-th entry.

Chapter 1

Introduction

In the realm of financial decision-making, the art of portfolio management stands as a cornerstone for investors seeking to optimize their investment strategies. The portfolio optimization problem, also known as asset allocation problem, presents a fascinating and complex challenge. In the modern world of finance, the foundational framework of Mean-Variance Portfolio (MVP) optimization (Markowitz, 1952) plays a pivotal role in portfolio optimization. MVP optimization casts the asset allocation problem as a convex optimization problem of finding optimal stock weights with two key inputs being expected returns and portfolio risk. By quantifying the trade-off between these two crucial dimensions, it empowers investors to make informed decisions that align with their risk preferences and financial goals.

The remainder of this thesis is organized as follows. In Section 1, we introduce the MVP optimization framework, a widely employed methodology for addressing the asset allocation problem. Section 2 presents an overview of 1-threshold Gerber correlation statistic, followed by an extension to accommodate an arbitrary number of thresholds, which, to the best of our knowledge, has not been previously developed. In Section 3, we present simulation results pertaining to the positive semi-definiteness properties of various Gerber correlation statistics. Section 4 offers a comprehensive performance evaluation comparing portfolios constructed based on 2- and 3-threshold Gerber correlation statistics with benchmark portfolios. Section 5 delves into another novel extension of Gerber correlation statistic, the time-varying Gerber correlation statistic that employs

1

the Exponentially Weighted Moving Average approach. Finally, in Section 6, we conclude our thesis by discussing the obtained results and providing recommendations for future research endeavors in this domain.

1.1 Portfolio Optimization Problem

The Mean-Variance Portfolio (MVP) optimization (Markowitz, 1952) is a classical problem in finance that seeks to determine the weight of different assets in a portfolio that maximizes the portfolio return subject to some constraints. The goal is to find the optimal portfolio weight that achieves the maximum possible return for a given level of portfolio variance.

The convex optimization problem for a portfolio of K stocks can be formulated as

$$
\begin{aligned}
\text{maximize } & \boldsymbol{w}^T \boldsymbol{\mu} \\
\text{subject to } & \boldsymbol{w}^T \boldsymbol{\Sigma} \boldsymbol{w} \leq \sigma^2_{target} \\
& \boldsymbol{w}^T \mathbf{1} = 1 \\
& 0 \leq w_i \leq 1, \ \ i = 1, \ldots, K
\end{aligned}
\tag{1.1}
$$

where $\boldsymbol{w}$ is a $K \times 1$ vector of weights representing the weight of each stock in the portfolio, $\boldsymbol{\mu}$ is a $K \times 1$ vector of expected returns that is representative of forecasted returns for the next time-stamp, $\boldsymbol{\Sigma}$ is a $K \times K$ covariance matrix of stock returns used as a measure of portfolio risk, σ^2_{target} is the maximum portfolio variance allowed, and $\mathbf{1}$ is a $K \times 1$ vector of ones.

The objective function represents the expected portfolio return achieved with weight $\boldsymbol{w}$. The constraints impose the weights add up to 1 and that the overall portfolio variance, which is the sum of the variances of each stock weighted by their respective weights and the covariance between assets, to be below a target variance level.

We can use a convex optimizer to solve for an optimal portfolio weight $\boldsymbol{w^*}$ that will maximize expected portfolio returns while achieving desired level of returns portfolio variance. The optimization problem can be repeatedly solved on a chosen frequency such

as daily, weekly, or monthly, and each time the portfolio can be re-balanced according to $\boldsymbol{w}^*$ to achieve optimal portfolio weights over time.

However, above formulation is unrealistic as it does not consider the transaction cost associated with re-balancing the portfolio each time the optimization problem is solved. Gerber et al. (2022) use the following modified MVP optimization formulation

$$
\begin{aligned}
\text{maximize} \quad & \boldsymbol{w}^T\boldsymbol{\mu} - \psi\,\mathbf{1}^T|\boldsymbol{w} - \boldsymbol{w}_0| \\
\text{subject to} \quad & \boldsymbol{w}^T\boldsymbol{\Sigma}\boldsymbol{w} \leq \sigma_{target}^2 \\
& \boldsymbol{w}^T\mathbf{1} = 1 \\
& 0 \leq w_i \leq 1, \;\; i = 1,\ldots,K
\end{aligned}
\tag{1.2}
$$

where $\psi\,\mathbf{1}^T|\boldsymbol{w} - \boldsymbol{w}_0|$ denotes a simplistic approximation of transaction cost (such as slippage and fees) associated with re-balancing the portfolio from previous weight $\boldsymbol{w}_0$ to new optimal weight $\boldsymbol{w}^*$. ψ is a fixed constant such as 10bps (0.1%). The transaction cost term in the objective helps to regulate portfolio turnover and encourages portfolio re-balancing that leads to high expected portfolio return with reduced associated costs.

Solving the optimization problem hinges on two fundamental inputs: the expected returns vector $\boldsymbol{\mu}$ and the covariance matrix of stock returns $\boldsymbol{\Sigma}$. Various approaches, ranging from simple historical averages and covariances to more sophisticated methods have been employed to model these inputs.

1.2 Modelling the Expected Returns

The first critical aspect of portfolio optimization revolves around the task of forecasting expected returns. Accurate predictions of asset performance serve as the bedrock upon which portfolio decisions are made. In this domain, a multitude of approaches have been proposed over the years. A common and simplest approach is by using the sample mean of historical returns over a fixed time horizon of length T. For example, the T-months historical mean returns can be used as a proxy for the expected return for the next month. Others delve into more sophisticated methods, embracing gradient boosted machines

(Roy et al., 2020) or deep-learning based techniques like LSTM networks (Yadav et al., 2020) to forecast the expected returns for the subsequent time-stamp.

For the purpose of this thesis, our primary focus lies elsewhere. We pivot our attention towards the intricacies of assessing risk in portfolio optimization, recognizing that effective risk modeling is pivotal for making informed investment decisions. We assume the use of simple historical returns for expected returns estimation, allowing us to allocate our resources more intensively towards understanding the complex nuances of risk modeling.

1.3   Modeling the Risk

The second critical facet of the portfolio optimization problem is modeling the risk component. Risk in portfolio optimization context encompasses various dimensions of uncertainty and market dynamics. At the heart is the task of capturing the co-movement relationships between assets within a portfolio. Effective risk modeling requires understanding how these assets move in relation to one another.

Some common approaches in modelling the risk include the use of a historical (sample) covariance matrix with lookback (rolling) window of length T, to more advanced techniques such as shrinkage covariance methods (Ledoit and Wolf, 2004) and modified covariance statistics such as the Gerber covariance (Gerber et al., 2022) statistic.

An alternative approach is to concurrently model the expected returns and the co-movement relationships among assets. To achieve this objective, the fusion of Copula theory (Nelsen, 2006) and Generalized Autoregressive Conditional Heteroskedasticity (GARCH) models has gained substantial attention. The Copula-GARCH model has been applied in MVP optimization settings (Sahamkhadam et al., 2018) or alternatively with the application of bootstrapping technique (Kresta, 2015). A distinguishing feature of Copula-GARCH models is their capacity to flexibly characterize tail dependencies, especially relevant for describing extreme events within financial markets, while also producing expected returns forecasts for the subsequent time-stamp. However, a drawback of this approach is its complex formulation and the computational overhead associated with extensive Monte Carlo simulations. This computational burden

renders Copula-GARCH models less practical, particularly when confronted with high-dimensional datasets.

In light of these considerations, this thesis takes a distinct path by centering its focus on the covariance matrix approach for modeling portfolio risk. Specifically, we explore the Gerber correlation statistic and the corresponding covariance matrix in describing asset co-movements as a simpler alternative. Gerber correlation is known to exhibit robustness against outliers and noise (Gerber et al., 2022). However, this robustness comes at a trade-off; while it excels in maintaining stability against noise and outliers, it does, in turn, exhibit a reduced capacity to capture the intricate tail-dependencies that become particularly crucial during extreme market events. To overcome this limitation, we introduce novel extensions to the Gerber correlation, thereby enhancing its flexibility in modeling tail-dependencies — a critical aspect in our pursuit of a more comprehensive and robust portfolio optimization strategy.

1.4 Co-movement measures

Co-movement measures play a crucial role in quantifying the dependence between variables. In particular, covariance and correlation measures have been universally adopted in finance in describing the dependence structure between different assets. In this section, we explore Pearson's correlation coefficient and Kendall's Tau, the two most widely known correlation measures.

1.4.1 Pearson's correlation coefficient

Pearson's correlation coefficient is the most widely used co-movement measure that describes the strength of linear relationship between two continuous random variables X and Y. Letting μ_Z and σ_Z to be the expected value and standard deviation of random variable Z, the population Pearson's correlation is defined as

$$\rho_{XY} = \frac{\text{Cov}(X, Y)}{\sqrt{\text{Var}(X)\text{Var}(Y)}} = \frac{E[(X - \mu_X)(Y - \mu_Y)]}{\sqrt{\text{Var}(X)\text{Var}(Y)}} =: \frac{\sigma_{XY}}{\sqrt{\sigma_X \sigma_Y}}. \tag{1.3}$$

As can be seen, Pearson's correlation is a standardized form of covariance that is independent of the units of measurement, with range being -1 to 1. Pearson's correlation

value of 1 (-1) means there exists a perfectly positive (negative) linear relationship between X and Y.

The sample (also referred to as historical) Pearson's correlation estimator that is used to estimate ρ_{XY} from a sample of n observations is

$$\hat{\rho}_{XY} = \frac{\sum_{i=1}^{n}(x_i - \bar{x})(y_i - \bar{y})}{\sqrt{\sum_{i=1}^{n}(x_i - \bar{x})^2 \sum_{i=1}^{n}(y_i - \bar{y})^2}}. \tag{1.4}$$

For a set of random variables $X_1, \ldots, X_K$, the correlation matrix $\boldsymbol{P}$ is defined as a $K \times K$ matrix whose (i, j)-th entry is

$$p_{ij} := \rho_{X_i X_j}. \tag{1.5}$$

Such correlation matrix can be estimated from a sample of observations by estimating the sample Pearson's correlation between each pair of variables using equation (1.4). Similarly, the covariance matrix $\boldsymbol{C}$ is defined as a $K \times K$ matrix whose (i, j)-th entry is $c_{ij} = \text{Cov(X,Y)}$. $\boldsymbol{C}$ can also be written in terms of the correlation matrix $\boldsymbol{P}$ as

$$\boldsymbol{C} = \text{diag}(\boldsymbol{\sigma})\,\boldsymbol{P}\,\text{diag}(\boldsymbol{\sigma}), \tag{1.6}$$

where $\boldsymbol{\sigma}$ is a $K \times 1$ vector of standard deviations for the K random variables, and $\text{diag}(\boldsymbol{\sigma})$ is a $K \times K$ diagonal matrix having $\boldsymbol{\sigma}$ as its diagonal entries. Given a valid correlation matrix, the corresponding covariance matrix can always be computed this way. Denoting the estimated correlation matrix as $\hat{\boldsymbol{P}}$, we can easily estimate the covariance matrix as $\hat{\boldsymbol{C}} := \text{diag}(\hat{\boldsymbol{\sigma}})\,\hat{\boldsymbol{P}}\,\text{diag}(\hat{\boldsymbol{\sigma}})$ where $\hat{\boldsymbol{\sigma}}$ is the $K \times K$ diagonal matrix of estimated standard deviations. When using the historical covariance matrix of asset returns as a measure of portfolio risk, $\hat{\boldsymbol{C}}$ will play the role of portfolio variance $\boldsymbol{\Sigma}$ in problem 1.2.

Despite the universal adoption of Pearson's correlation to describe linear dependence between random variables, there exist several drawbacks, some of which are outlined by Aggarwal and Ranganathan (2016). Firstly, Pearson's correlation is only best applied to data that follow a normal distribution and when the relationship between variables is linear. Secondly, it only applies to data on a continuous scale. Other measures of co-movement such as non-parametric correlation measures like Kendall's Tau should be used in other cases. Thirdly, the presence of outliers can severely distort the estimated correlation value due to the product-moment terms, as seen in the numerator of equation

(1.4). The third is the most critical drawback of using Pearson's correlation in portfolio optimization framework as financial data often exhibit heavy tails.

1.4.2 Kendall's Tau

The Kendall rank correlation coefficient (Kendall, 1938), also referred to as Kendall's Tau correlation, is another measure of co-movement used to assess the strength of the monotonic association between two random variables. Calculations are based on the notion of concordant and discordant pairs and Kendall's Tau can be used on both continuous and ordinal data. Kendall's Tau is a non-parametric correlation measure as it does not place any distributional assumptions on the data.

Letting $(x_1, y_1), \ldots, (x_n, y_n)$ be a set of observations of two random variables X and Y, a pair of observations (x_i, y_i) and (x_j, y_j) is said to be *concordant* if $x_i > x_j$ and $y_i > y_j$, or $x_i < x_j$ and $y_i < y_j$. The pair is *discordant* if $x_i > x_j$ and $y_i < y_j$, or $x_i > x_j$ and $y_i < y_j$.

Kendall's Tau between X and Y is then calculated as

$$\tau_{XY} = \frac{\text{(Number of concordant pairs)} - \text{(Number of discordant pairs)}}{\text{Number of pairs}} \tag{1.7}$$

$$=: \frac{n_{XY}^c - n_{XY}^d}{n_{XY}^d + n_{XY}^d}. \tag{1.8}$$

There are further adjustments made for discrete data in case of ties when $x_i = x_j$ or $y_i = y_j$ (Agresti, 2010).

Most notable properties of Kendall's Tau include

- The range is -1 to 1.

- If X and Y are independent and not constant, then the expectation of correlation is zero.

- Kendall's Tau of 1 (-1) means the agreement (disagreement) is perfect.

Key advantages of Kendall's Tau over Pearson's correlation lie in its non-parametric nature, liberating itself from distributional assumptions and robustness against extreme outliers.

1.4.3   Positive semi-definiteness

For a set of random variables $X_1, \ldots, X_K$, we can estimate the pair-wise correlation using a given estimation method such as Pearson's correlation or Kendall's Tau, and form a $K \times K$ correlation matrix.

Positive semi-definiteness is an important characteristic of correlation (and covariance) matrices. A $K \times K$ symmetric real matrix $\boldsymbol{M}$ is said to be positive semi-definite if $\boldsymbol{x}^T \boldsymbol{M} \boldsymbol{x} \geq 0$ for all $\boldsymbol{x} \in \mathbb{R}^K$, whereas a $K \times K$ symmetric real matrix $\boldsymbol{M}$ is said to be positive definite if $\boldsymbol{x}^T \boldsymbol{M} \boldsymbol{x} > 0$ for all $\boldsymbol{x} \in \mathbb{R}^K \setminus \{\boldsymbol{0}\}$. Equivalently, a real, symmetric matrix is positive semi-definite (definite) if and only if all its eigenvalues non-negative (positive).

A famous result regarding positive semi-definiteness is that the covariance (and therefore correlation) of a multivariate probability distribution is always positive semi-definite, and is positive definite unless one variable is an exact linear function of others. Conversely, any matrix that satisfies the positive semi-definite property can be considered as the covariance matrix of some multivariate distribution. Hence, any new measure of correlation that is developed must ensure the property that the correlation matrix is positive semi-definite.

Also, any $K \times K$ correlation matrix fully comprised of pairwise Pearson's correlations or Kendall's Tau correlations is positive semi-definite, thus they are valid measures of correlation between random variables.

Chapter 2

Gerber correlation

The Gerber correlation statistic (Gerber et al., 2022) is a robust co-movement measure for correlation matrix estimation specifically used in portfolio construction settings. It resembles Kendall's Tau in that it uses the notion of concordance and discordance of random variables to define the strength of co-movement. Gerber correlation achieves robustness as it is not severely affected by extremely small or large movements, which often represent noise in financial data.

2.1   1-threshold Gerber correlation

We denote the original Gerber correlation statistic developed by Gerber et al. (2022) the *1-threshold Gerber correlation.*

Let r_{tk} be the return of asset k at time t, for $k = 1, \ldots, K$ assets and $t = 1, \ldots, T$ time periods. For every pair (i, j) of assets for each time t, we give a co-movement weight to the pair of returns observation (r_{ti}, r_{tj}) with the weight function $m_{ij}(t)$ defined as

$$
m_{ij}(t) = \begin{cases}
+1 & r_{ti} \geq +H_i, \ r_{tj} \geq +H_j \\
+1 & r_{ti} < -H_i, \ r_{tj} < -H_j \\
-1 & r_{ti} \geq +H_i, \ r_{tj} < -H_j \\
-1 & r_{ti} < -H_i, \ r_{tj} \geq +H_j \\
0 & \text{otherwise}
\end{cases}
\tag{2.1}
$$

where $H_k \geq 0$ is asset-specific threshold that defines the distinct regions of co-movements. We usually set $H_k = cs_k$ with c being some non-negative fraction (typically $1/2$) and s_k being the sample standard deviation of the return of asset k. Setting a single threshold of $H_k = c$ will have the equivalent effect of having $H_k = cs_k$ as we can standardize each time-series to have variance equal to 1 with the transformation $\frac{r_{tk} - \bar{r}_k(t)}{\sigma_k(t)}$ for each asset k where $\bar{r}_k(t)$ and $\sigma_k(t)$ represent the mean and standard deviation of returns of asset k observed at time t, respectively,

The weight assigning function $m_{ij}(t)$ for 1-threshold Gerber correlation defines 4 discrete regions of non-zero co-movement weights. We refer to those pairs with $m_{ij}(t) = 1$ as a *concordant* pair and those with $m_{ij}(t) = -1$ as a *discordant* pair. A pair of asset returns with at least one asset return being below their respective threshold is given a co-movement weight of 0, i.e., regarded as noise and ignored in correlation computation.

Figure 2.1 shows examples of $m_{ij}(t_0)$ values on the z-axis, at an arbitrary time-stamp t_0, obtained by varying the threshold H. These are the co-movement weights assigned with $m_{ij}(t_0)$. The two axes named X and Y can be thought as the axes for standardized returns series for two assets. Sensitivity to tails and degree of asymmetry are controlled with the choice of threshold values H_i.

FIGURE 2.1: Example $m_{ij}(t_0)$ function values for varying values of threshold H for return series X and Y. **Left:** Common threshold H of 0 for both series. **Middle:** Common threshold H of 0.5 for both series. **Right:** thresholds of 0.3 and 1.5 for X and Y, respectively.
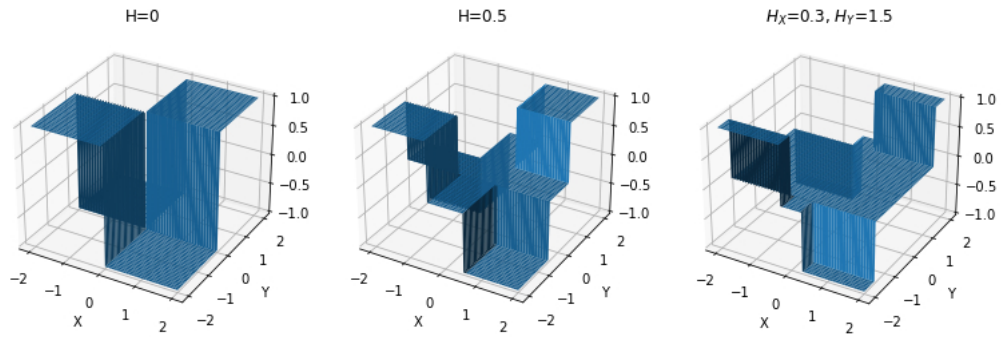
Gerber et al. (2022) define their initial version of Gerber correlation between assets i and j as

$$g_{ij} = \frac{\sum_{t=1}^{T} m_{ij}(t)}{\sum_{t=1}^{T} |m_{ij}(t)|} = \frac{n_{ij}^c - n_{ij}^d}{n_{ij}^c + n_{ij}^d} \tag{2.2}$$

where n_{ij}^c is the number of concordant pairs for series i and j and n_{ij}^d is the number of discordant pairs. Note the resemblance between equation (2.2) and Kendall's Tau in

equation (1.8). They only differ in how the notion of concordance and discordance are defined.

Gerber correlation in (2.2) relies only on the counts of simultaneous piercings of the thresholds and not on the extent to which the thresholds are pierced. Thus, it is insensitive to extreme large movements that may otherwise distort the estimation process. It is also insensitive to small movements that may simply be noise as these movements get filtered out with assigned weight $m_{ij}(t)$ of 0.

However, Gerber et al. (2022) state that the denominator in (2.2) must be altered to obtain a Gerber correlation (and covariance) matrix that is positive semi-definite. Formulation of Gerber correlation in (2.2) has found to be not always positive semi-definite. The alternative formulation that yields a positive semi-definite Gerber correlation matrix is

$$g_{ij} = \frac{\sum_{t=1}^{T} m_{ij}(t)}{T - n_{ij}^{NN}} = \frac{n_{ij}^c - n_{ij}^d}{T - n_{ij}^{NN}} \tag{2.3}$$

where $n_{ij}^{NN} := |\{(i,j) : |r_{ti}| < H_i, |r_{tj}| < H_j \text{ where } t = 1, \ldots, T\}|$, i.e. the number of observations for which the absolute value of returns for assets i and j are less than H_i and H_j, respectively. Gerber et al. (2023) provide the complete proof of positive semi-definiteness of 1-threshold Gerber correlation. Note, depending on the data, setting thresholds H_j's too high may lead to $T - n_{ij}^{NN} = 0$ for some pairs of assets and hence an undefined Gerber correlation g_{ij}. We should always avoid this situation and this can be achieved by setting appropriate threshold values.

Gerber et al. (2022) show in their empirical study that using 1-threshold Gerber covariance matrix in portfolio optimization setting outperformed against using the historical covariance matrix and the shrinkage estimator of Ledoit and Wolf (2004) in most scenarios, during the period of January 1988 to December 2020 on a well diversified portfolio of 9 assets.

2.2 2-threshold Gerber correlation

We develop an extension to the 1-threshold Gerber correlation by introducing another level of threshold so that we have two upper and lower thresholds, resulting in up to 16 discrete regions with non-zero co-movement weights. Our motivation is that such finer

division of weight-assigned regions can help us to define finer levels of concordance and discordance. As financial data often exhibits heavy tails, we believe assigning uniform weight of ± 1 to all points that are not filtered out, as in 1-threshold Gerber correlation, may not flexibly describe the degree of co-movements in the tails.

The co-movement weight function $m_{ij}(t)$ for the 2-threshold Gerber correlation is defined as

$$
m_{ij}(t) = \begin{cases}
+1 & r_{ti} \geq Q, r_{tj} \geq Q \\
+1 & r_{ti} < -Q, r_{tj} < -Q \\
+1 & P \leq r_{ti} < Q, P \leq r_{tj} < Q \\
+1 & -Q \leq r_{ti} < -P, -Q \leq r_{tj} < -P \\
+\alpha & r_{ti} \geq Q, P \leq r_{tj} < Q \\
+\alpha & r_{ti} < -Q, -Q \leq r_{tj} < -P \\
+\alpha & P \leq r_{ti} < Q, r_{tj} \geq Q \\
+\alpha & -Q \leq r_{ti} < -P, r_{tj} < -Q \\
-\alpha & r_{ti} \geq Q, -Q \leq r_{tj} < -P \\
-\alpha & r_{ti} < -Q, P \leq r_{tj} < Q \\
-\alpha & -Q \leq r_{ti} < -P, r_{tj} \geq Q \\
-\alpha & P \leq r_{ti} < Q, r_{tj} < -Q \\
-1 & r_{ti} \geq Q, r_{tj} < -Q \\
-1 & r_{ti} < -Q, r_{tj} \geq Q \\
-1 & P \leq r_{ti} < Q, -Q \leq r_{tj} < -P \\
-1 & -Q \leq r_{ti} < -P, P \leq r_{tj} < Q \\
0 & \text{otherwise}
\end{cases}
\tag{2.4}
$$

where $0 \leq P \leq Q$ are the two thresholds, α is the co-movement weight given to points with partial co-movement defined via P and Q. It makes logical sense to have $0 \leq \alpha \leq 1$ but later we show mathematically that α can be negative and still result in a positive semi-definite correlation matrix. Thresholds P and Q are non-negative constants for all series unlike the series-dependent thresholds for 1-threshold Gerber correlation. This is not a problem under the assumption that the returns time series have been standardized to have variance 1 and mean 0.

Refer to a pair with $m_{ij}(t) = 1$ as a fully-concordant pair, $m_{ij}(t) = \alpha$ as a partially-concordant pair, $m_{ij}(t) = -1$ as a fully-discordant pair, and $m_{ij}(t) = -\alpha$ as a partially-discordant pair.

Fully concordant pairs are those that simultaneously pierce the larger threshold Q or $-Q$, or those that are simultaneously between P and Q or between $-Q$ and $-P$. Partially concordant pairs are those where only one pierces through the larger threshold Q or $-Q$ and the other is between P and Q or $-Q$ and $-P$. Fully and partially discordant pairs have similar conditions but where the sign of one point is opposite of the other.

In two special cases, when $\alpha = 1$ or when $P = Q$, the weight assigning function $m_{ij}(t)$ of 2-threshold Gerber correlation reduces to that of original 1-threshold Gerber correlation with common threshold Q, and the resulting $m_{ij}(t)$ function values are identical.

Figure 2.2 shows three examples of $m_{ij}(t_0)$ function values for varying α between 0 and 1. We see that introducing an additional threshold has enabled greater flexibility in how we can define the co-movement regions. For $\alpha = 0.5$, there are now 16 regions with non-zero co-movement weight $m_{ij}(t_0)$ values, where the magnitude of co-movement decays from 1 to α as the pair of returns move further away from *principal diagonals* (diagonal from top-right to bottom-left passing through the origin). In addition, as noted above, when $\alpha = 1$ function values are identical to that from 1-threshold Gerber correlation with thresholds $H_x = 0.2$ and $H_y = 0.7$.

FIGURE 2.2: Example $m_{ij}(t_0)$ function values for varying values α and fixed $P = 0.2$, $Q = 0.7$. **Left:** $\alpha = 0$. **Middle:** $\alpha = 0.5$. **Right:** $\alpha = 1$.
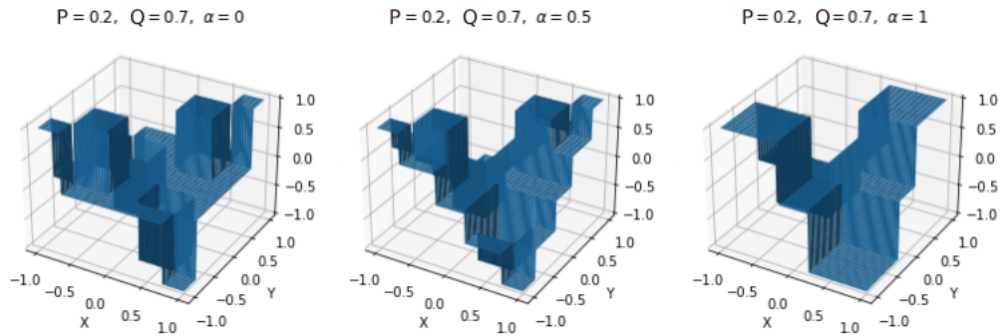
Similar to 1-threshold Gerber correlation, defining the 2-threshold Gerber correlation as in equation (2.2) does not guarantee positive semi-definiteness of the correlation matrix. Following the similar formulation of 1-threshold Gerber correlation as in equation (2.3)

we define the positive semi-definiteness guaranteed 2-threshold Gerber correlation as

$$g_{ij} = \frac{\sum_{t=1}^{T} m_{ij}(t)}{T - n_{ij}^{NN}} \tag{2.5}$$

where the numerator sums all weights of fully and partially concordant and discordant pairs and n_{ij}^{NN} is the number of observations for which both of asset returns of i and j lie between the smaller thresholds $-P$ and P (i.e., $n_{ij}^{NN} := |\{(i,j) \ : \ |r_{ti}| < P, \ |r_{tj}| < P$ where $t = 1, \ldots, T\}|$). As in the case for 1-threshold Gerber correlation, the choice P must not be too large to ensure $T - n_{ij}^{NN} \neq 0$.

We denote $\boldsymbol{G}$ as the Gerber correlation matrix with entries g_{ij}. In Appendix A.1 we prove positive semi-definiteness of the numerator matrix of 2-threshold Gerber correlation matrix.

2.3 $\ 3$-threshold Gerber correlation

Going further, we develop the 3-threshold Gerber correlation statistic with three threshold levels C_1, C_2, C_3 in increasing magnitude and $\alpha_1, \alpha_2, \alpha_3$ as the weights given to the regions with varying strengths of co-movement. In this thesis, we always fix $\alpha_1 = 1$. Compared to the 2-threshold Gerber correlation, there is an additional threshold C_3 and weight α_3 introduced. This results in up to 36 non-zero co-movement weight-assigned regions used to compute the correlation measure.

The co-movement weight function $m_{ij}(t)$ for a pair of standardized returns (r_{ti}, r_{tj}) is defined as

$$m_{ij}(t) = \begin{cases} +1 & \pm r_{ti} \geq C_3, \quad \pm r_{tj} \geq C_3 \\ +1 & C_s \leq \pm r_{ti} < C_{s+1}, C_s \leq \pm r_{tj} < C_{s+1} \\ & \quad \text{for } s = 1, 2 \\ +\alpha_2 & \pm r_{ti} \geq C_3, C_2 \leq \pm r_{tj} < C_3 \\ +\alpha_2 & C_2 \leq \pm r_{ti} < C_3, \pm r_{tj} \geq C_3 \\ +\alpha_2 & C_2 \leq \pm r_{ti} < C_3, C_1 \leq \pm r_{tj} < C_2 \\ +\alpha_2 & C_1 \leq \pm r_{ti} < C_2, C_2 \leq \pm r_{tj} < C_3 \\ +\alpha_3 & \pm r_{ti} \geq C_3, \quad C_1 \leq \pm r_{tj} < C_2 \\ +\alpha_3 & C_1 \leq \pm r_{ti} < C_2, \quad \pm r_{tj} \geq C_3 \\ -\alpha_3 & \mp r_{ti} \geq C_3, \quad C_1 \leq \pm r_{tj} < C_2 \\ -\alpha_3 & C_1 \leq \mp r_{ti} < C_2, \quad \pm r_{tj} \geq C_3 \\ -\alpha_2 & \mp r_{ti} \geq C_3, C_2 \leq \pm r_{tj} < C_3 \\ -\alpha_2 & C_2 \leq \mp r_{ti} < C_3, \pm r_{tj} \geq C_3 \\ -\alpha_2 & C_2 \leq \mp r_{ti} < C_3, C_1 \leq \pm r_{tj} < C_2 \\ -\alpha_2 & C_1 \leq \mp r_{ti} < C_2, C_2 \leq \pm r_{tj} < C_3 \\ -1 & \mp r_{ti} \geq C_3, \quad \pm r_{tj} \geq C_3 \\ -1 & C_s \leq \mp r_{ti} < C_{s+1}, C_s \leq \pm r_{tj} < C_{s+1} \\ & \quad \text{for } s = 1, 2 \\ 0 & \text{otherwise} \end{cases} \tag{2.6}$$

where $0 \leq C_1 \leq C_2 \leq C_3$ for the thresholds.

Note we write the conditions in a compact format. For example, $\pm r_{ti} \geq C_3, \quad \pm r_{tj} \geq C_3$ refers to two separate conditions $r_{ti} \geq C_3, \quad r_{tj} \geq C_3$ and $-r_{ti} \geq C_3, \quad -r_{tj} \geq C_3$, i.e., the top-right and bottom-left regions with weight $\alpha_1 = 1$ as illustrated in Figure 2.3.

In Appendix A.2 we derive a sufficient condition for the values of α_2 and α_3 for positive semi-definiteness of the 3-threshold Gerber correlation matrix. These conditions are as follows

$$\begin{cases} |\alpha_2| < 1 \\ \alpha_3 < 1 \\ \alpha_3 + 1 > 2\alpha_2^2. \end{cases} \tag{2.7}$$

Figure A.1 shows visually the feasible region for α_2 and α_3.

Given the above constraints, the 3-threshold Gerber correlation matrix with entries

$$g_{ij} = \frac{\sum_{t=1}^{T} m_{ij}(t)}{T - n_{ij}^{NN}} \tag{2.8}$$

is guaranteed to be positive semi-definite. Note $n_{ij}^{NN} := |\{(i, j) \; : \; |r_{ti}| < C_1, \; |r_{tj}| < C_1$ where $t = 1, \ldots, T\}|$.

FIGURE 2.3: Illustration of co-movement weight regions for 3-threshold Gerber correlation. The returns pair (r_{ti}, r_{tj}) will be plotted as a point with x and y coordinates, then mapped to a weight value using $m_{ij}(t)$. Grey region denotes weight values of 0.
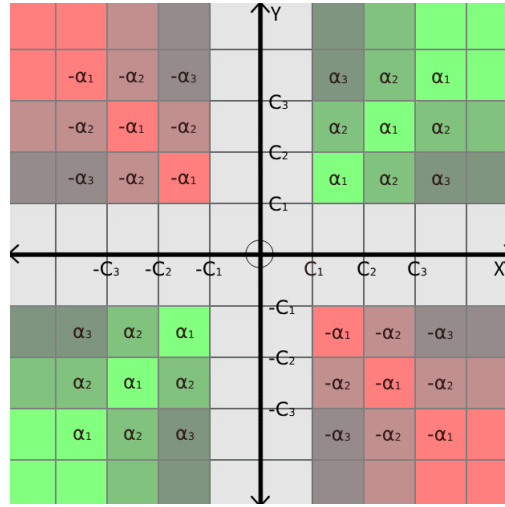
2.4 n-threshold Gerber correlation

n-threshold Gerber correlation $(n \geq 2)$ is the generalization of Gerber correlation statistic with n discrete thresholds that allows us to define up to $4n^2$ discrete regions of non-zero co-movement weights. The 2-threshold and 3-threshold Gerber correlations presented in previous sections are examples of n-threshold Gerber correlation statistic.

The co-movement weight assigning function $m_{ij}(t)$ for n-threshold Gerber correlation is defined by n weights $\alpha_1, \ldots, \alpha_n$ (with $\alpha_1 = 1$ fixed) and n thresholds $C_1, \ldots, C_n$ that together determine the varying co-movement regions created with $m_{ij}(t)$. The weight assigning function $m_{ij}(t)$ for n-threshold Gerber correlation statistic is defined as

$$
m_{ij}(t) = \begin{cases}
+1 & \pm r_{ti} \geq C_n, \quad \pm r_{tj} \geq C_n \\
+1 & C_s \leq \pm r_{ti} < C_{s+1}, C_s \leq \pm r_{tj} < C_{s+1} \\
& \quad \text{for } s = 1, \ldots, n-1 \\
+\alpha_l & \pm r_{ti} \geq C_n, C_{n-l+1} \leq \pm r_{tj} < C_{n-l+2} \\
+\alpha_l & C_{n-l+1} \leq \pm r_{ti} < C_{n-l+2}, \pm r_{tj} \geq C_n \\
+\alpha_l & C_s \leq \pm r_{ti} < C_{s+1}, C_{s-1} \leq \pm r_{tj} < C_s \\
& \quad \text{for } s = l, \ldots, n-1 \text{ if } l \geq n-1 \\
+\alpha_l & C_{s-1} \leq \pm r_{ti} < C_s, C_s \leq \pm r_{tj} < C_{s+1} \\
& \quad \text{for } s = l, \ldots, n-1 \text{ if } l \geq n-1 \\
-\alpha_l & \mp r_{ti} \geq C_n, C_{n-l+1} \leq \pm r_{tj} < C_{n-l+2} \\
-\alpha_l & C_{n-l+1} \leq \mp r_{ti} < C_{n-l+2}, \pm r_{tj} \geq C_n \\
-\alpha_l & C_s \leq \mp r_{ti} < C_{s+1}, C_{s-1} \leq \pm r_{tj} < C_s \\
& \quad \text{for } s = l, \ldots, n-1 \text{ if } l \geq n-1 \\
-\alpha_l & C_{s-1} \leq \mp r_{ti} < C_s, C_s \leq \pm r_{tj} < C_{s+1} \\
& \quad \text{for } s = l, \ldots, n-1 \text{ if } l \geq n-1 \\
-1 & \mp r_{ti} \geq C_n, \quad \pm r_{tj} \geq C_n \\
-1 & C_s \leq \mp r_{ti} < C_{s+1}, C_s \leq \pm r_{tj} < C_{s+1} \\
& \quad \text{for } s = 1, \ldots, n-1 \\
0 & \text{otherwise}
\end{cases}
\tag{2.9}
$$

where $l = 2, \ldots, n$ and $0 \leq C_1 \leq \ldots \leq C_n$.

Figure 2.4 illustrates bird-eye view of values assigned with $m_{ij}(t)$ of n-threshold Gerber correlation statistic.

In previous sections we saw positive semi-definiteness of 1-, 2- and 3-threshold Gerber correlation statistics with appropriate conditions on the co-movement weights where necessary.

We define the n-threshold Gerber correlation between returns of assets i and j as

$$
g_{ij} = \frac{\sum_{t=1}^{T} m_{ij}(t)}{T - n_{ij}^{NN}}.
\tag{2.10}
$$

In Appendix A.3 we derive a sufficient condition for positive semi-definiteness of n-threshold Gerber correlation matrix for any $n \geq 2$.

FIGURE 2.4: Illustration of co-movement weight regions for n-threshold Gerber correlation. The returns pair (r_{ti}, r_{tj}) will be plotted as a point with x and y coordinates, then mapped to a weight value using $m_{ij}(t)$. Grey region denotes weight values of 0.
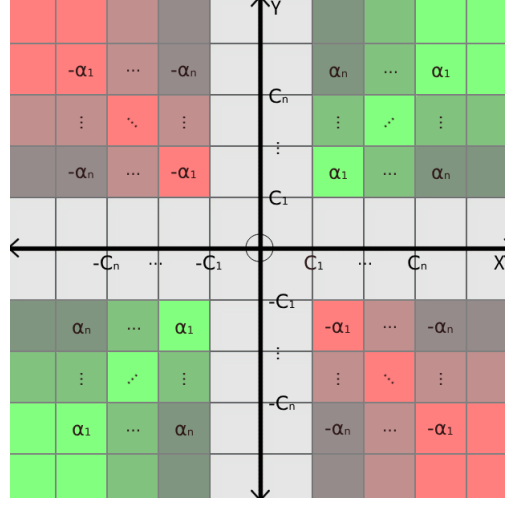
2.5 Tanh-tanh Gerber correlation

In an attempt to develop a continuous analogue of Gerber correlation statistic, we introduce the tanh-tanh Gerber correlation statistic.

The co-movement weight assigning tanh-tanh Gerber correlation is defined as

$$m_{ij}(t) = \tanh\left(a(r_{ti} - c)\right)\tanh(b(r_{tj} - d)). \tag{2.11}$$

The tanh-tanh co-movement weight function shares certain desirable properties as the Gerber correlation statistic. It maintains a bounded range within -1 and 1. Furthermore, it allows us to flexibly specify the degree of co-movement between distinct (r_{ti}, r_{tj}) coordinates, similarly to the discrete n-threshold Gerber correlation statistics, albeit in a continuous fashion. In addition, the slope parameters a and b enable us to control the rate at which the transition from weak to strong co-movement occurs, i.e., sensitivity to the tails. Moreover, it grants us the capability to better model asymmetry in asset returns with horizontal shift parameters c and d. These tunable parameters allow us to fine-tune the weight function's behavior and adapt it to various empirical scenarios.

Figure 2.5 shows examples of $m_{ij}(t_0)$ values on the z-axis, at an arbitrary time-stamp t_0, obtained by varying the parameters. The two axes named X and Y can be thought as the axes for standardized returns series for two assets.

FIGURE 2.5: Illustration of co-movement weight values for tanh-tanh Gerber correlation.
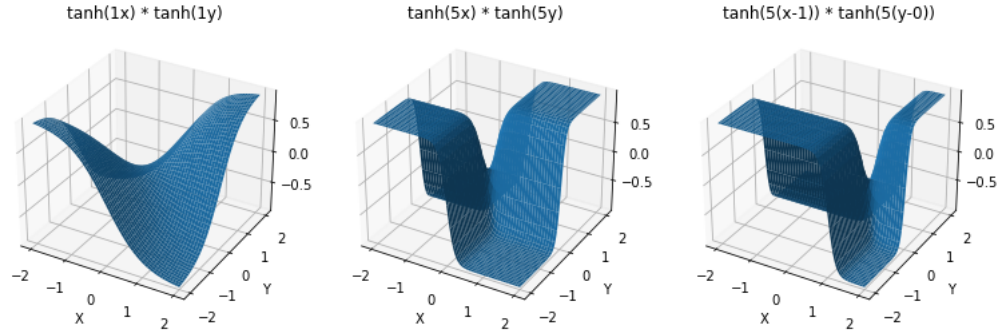
The tanh-tanh Gerber correlation does not have a cross-like region with $m_{ij} = 0$ for filtering out certain returns pairs as noise, however it assigns decreasing weights in a continuous manner. Hence, we define the tanh-tanh Gerber correlation as

$$g_{ij} = \frac{\sum_{t=1}^{T} m_{ij}(t)}{\sum_{t=1}^{T} |m_{ij}(t)|}. \tag{2.12}$$

Chapter 3

Simulation study

In this section we perform simulations to explore and verify some of the theoretical properties regarding positive semi-definiteness of various forms of Gerber correlation introduced.

3.1 Simulation Setup

We generate synthetic but realistic time-series stock returns data to verify whether different versions of Gerber correlation matrices introduced are positive semi-definite or not. This is to verify that Gerber correlation matrices computed using equation 2.2 are indeed sometimes not positive semi-definite and hence not suitable for use. We also verify positive semi-definiteness of Gerber correlation matrices computed using the modified denominator of $T - n_{ij}^{NN}$.

1. Set values of relevant parameters for the threshold and weights, depending on the type of Gerber correlation used.

2. Randomly pick K constituent stocks from S&P500 in 2022 and retrieve their log returns data between 2012-01-01 and 2022-12-31, where log return $r_{tk} = \log \frac{P_{tk}}{P_{t-1,k}}$

3. Compute the sample Pearson correlation matrix $\mathbf{\Sigma}$ of the data to use as the true correlation matrix of data generating process.

4. Sample T observations from $N_K(\mathbf{0}, \mathbf{\Sigma})$.

5. Compute Gerber correlation matrix using a choice of formula on the T observations.

6. Check for positive semi-definiteness of Gerber correlation matrix by verifying all eigenvalues of the matrix are real and non-negative.

7. For varying types of Gerber correlation metrics (e.g., 1-threshold, 2-threshold, etc.), repeat steps 1 to 6 R times and record the number of trials with positive semi-definite Gerber correlation matrix.

For all simulations below, we fix $K = 20$, $T = 1000$ and $R = 1000$.

3.2   1-threshold Gerber correlation

We empirically verify that the 1-threshold Gerber correlation is positive semi-definite in the general case with the modified denominator $T - n_{ij}^{NN}$, where Gerber et al. (2023) already proved positive semi-definiteness in writing. The non-positive semi-definite nature of 1-threshold Gerber correlation as defined in (2.2) is also verified.

In Table 3.1 we show the number of positive semi-definite Gerber correlation matrices out of 1000 repetitions. As already mentioned, Gerber correlation defined as in equation (2.2) yields non-positive definite matrices for some settings of thresholds H, whereas equation (2.3) always leads to positive semi-definiteness regardless of H.

TABLE 3.1: Simulation results showing number of repetitions with positive semi-definite correlation matrices for two versions of denominators for 1-threshold Gerber correlation. Common threshold value H is used if H_k is not specified.

Thresholds	(2.2)	(2.3)
$H = 2$	1	1000
$H = 1$	0	1000
$H = 0.5$	15	1000
$H = 0$	1000	1000
$H_k = 0.05(k - 1),$ $k = 1, \ldots, K$	1	1000
$H_k = 1 - 0.05(k - 1)$ $k = 1, \ldots, K$	0	1000

TABLE 3.2: Simulation results showing number of repetitions with positive semi-definite correlation matrices for 2-threshold Gerber correlation as defined in (2.5). Common thresholds of $P = 0.5$ and $Q = 1$ used for all assets $k = 1, \ldots, K$ as positive semi-definiteness is affected by α only.

Weights	Positive semi-definite matrices
$\alpha = 3$	165
$\alpha = 2$	1000
$\alpha = 1$	1000
$\alpha = 0.5$	1000
$\alpha = 0$	1000
$\alpha = -0.5$	1000
$\alpha = -1$	1000
$\alpha = -2$	70
$\alpha = -3$	0

3.3 2-threshold Gerber correlation

In Appendix A.1 we show that $|\alpha| \leq 1$ is a sufficient condition for 2-threshold Gerber correlation to be positive semi-definite. The two thresholds P and Q do not play a direct role in determining positive semi-definiteness of the correlation matrix, except that the choice of P must ensure that $T - n_{ij}^{NN} \neq 0$.

We perform the simulation study described above again to empirically verify positive semi-definiteness of 2-threshold Gerber correlation matrices computed using equation 2.5, but this time with varying α that controls the weight assigned to data points that are partially concordant or discordant. We do not include the results for 2-threshold Gerber correlation matrices with unmodified denominator as we have already seen for 1-threshold Gerber correlation it is not positive semi-definite in many cases.

Table 3.2 shows that the sufficient condition of $|\alpha| \leq 1$ for positive semi-definiteness holds. However, we see it is not a necessary condition as for example $\alpha = 2$ also yielded 1000 positive semi-definite Gerber correlation matrices.

3.4   3-threshold Gerber correlation

In Appendix A.2 we derive that

$$
\begin{cases}
|\alpha_2| < 1 \\
\alpha_3 < 1 \\
\alpha_3 + 1 > 2\alpha_2^2
\end{cases}
$$

is a sufficient condition for positive semi-definiteness of 3-threshold Gerber correlation statistic. We vary α_2 and α_3 to be within and outside the feasible region (illustrated in Figure A.1) and verify whether the 3-threshold Gerber correlation with modified denominator satisfies positive semi-definiteness. Table B.1 shows the results. Indeed, when α_2 and α_3 satisfy the sufficient condition 2.7, we always obtain 1000 positive semi-definite matrices. When the sufficient condition is not satisfied, we have some scenarios where we obtain 0, some positive number, or 1000 positive semi-definite matrices.

3.5   Tanh-tanh Gerber correlation

Table B.2 presents the count of positive semi-definite matrices observed over 100 repetitions for each distinct configuration characterized by the parameters (a, b, c, d). Notably, none of the parameter settings yielded a 100% occurrence of positive semi-definite matrices. This empirical evidence suggests that the tanh-tanh Gerber correlation, as defined in Section 2.5, does not consistently exhibit the property of being positive semi-definite. This suggests an intriguing avenue for future research. Specifically, it raises the question of whether the introduction of a region in which data points are considered noise and assigned a weight of 0, akin to the n-threshold Gerber correlation statistics, could potentially render the correlation matrix positive semi-definite.

Chapter 4

Empirical study

This chapter presents an empirical study that investigates the performance of 2-threshold Gerber covariance matrix in portfolio optimization context, and compares it to using the original 1-threshold Gerber covariance and the widely used historical covariance as benchmarks.

4.1 Nine assets

The data used in this study comprises a diversified collection of nine assets, spanning the time period from January 2012 to December 2022. The assets included in the data are as follows:

1. S&P 500 index: This index represents U.S. large-cap stocks.

2. Russell 2000 index: This index represents U.S. small-cap stocks.

3. MSCI EAFE index: This index encompasses large and mid-cap equities across twenty-one developed countries, excluding the U.S. and Canada.

4. MSCI Emerging Markets index: This index represents large and mid-cap equities across twenty-seven emerging markets.

5. iShares Core US Aggregate Bond ETF: Tracks the investment results of an index composed of the total U.S. investment-grade bond market.

6. iShares iBoxx $ High Yield Corporate Bond ETF: Tracks the investment results of an index composed of U.S. dollar-denominated, high yield corporate bonds.

7. Real estate FTSE NAREIT all equity REITS index: Captures the performance of real estate investment trusts.

8. Gold: Represents the price of gold.

9. S&P GSCI Goldman Sachs Commodity index: This index tracks the performance of a broad range of commodities.

We used Yahoo Finance to obtain the daily close prices (after adjustments for all applicable splits and dividend distributions) of these assets. We referred to Gerber et al. (2022) for the empirical study set-up, including the list of 9 assets and backtesting procedure. Note we could not acquire publicly available data for original assets 5 and 6 from their empirical study, hence replaced with assets 5 and 6 shown above that are ETFs that track the same underlying quantities.

4.1.1 Backtesting procedure

An example of portfolio backtesting procedure for comparing performances of different covariance matrix types using the above data described is as follows:

1. Set re-balancing frequency (e.g., monthly) and lookback window L (e.g., 12) for which the estimation of the expected returns $\boldsymbol{\mu}$ and covariance matrix (for the chosen estimation method) $\boldsymbol{\Sigma}$ will be based on.

2. Set the values of other parameters like the transaction cost term ψ, portfolio variance target σ_{target}^2 and Gerber-specific parameters like threshold values H_i for 1-threshold Gerber correlation, and P, Q and α for 2-threshold Gerber correlation, etc.

3. Asset returns data, at chosen re-balancing frequency, are retrieved for the period January 2012 to December 2022. Returns are calculated as percentage differences, $r_{t,i} = \frac{price_t}{price_{t-1,i}} - 1$.

4. Returns data of K assets for the first L time-stamps, i.e., $\boldsymbol{r}_t := (r_{t1}, \ldots, r_{tK})$ for $t = 1, \ldots, L$ are then standardized with $\hat{\boldsymbol{r}}_t := (\hat{r}_{t1}, \ldots, \hat{r}_{tK})$ where $\hat{r}_{tk} = \frac{r_{tk} - \bar{r}_k(t)}{\sigma_k(t)}$, which is used to compute $\boldsymbol{\mu} = \frac{1}{L} \sum_{t=1}^{t=L} \hat{\boldsymbol{r}}_t$ and covariance matrix $\boldsymbol{\Sigma}$ for the chosen estimation method. $\boldsymbol{\Sigma}$ is estimated by first computing the correlation matrix using chosen estimation method, then with equation 1.6.

5. Solve the convex optimization problem 1.2 by substituting $\boldsymbol{\mu}$ and $\boldsymbol{\Sigma}$ and find the optimal portfolio weight for the next time-stamp $\boldsymbol{w}_{L+1}^*$ given maximum allowed portfolio variance σ_{target}^2.

6. Re-balance the portfolio according to $\boldsymbol{w}_{L+1}^*$ and hold it for next unit of time-stamp. At the end of the holding period, calculate portfolio returns with $\boldsymbol{w}_{L+1}^{*T} \tilde{\boldsymbol{r}}_{L+1}$ where $\tilde{\boldsymbol{r}}_{L+1}$ is the realized asset returns for the time-stamp $L + 1$.

7. Repeat steps 4 to 6 by shifting the lookback period one time-stamp forward each time. Each time the *training* period will shift forward by 1 time-stamp so we have a constant lookback window of length L.

8. Compute various portfolio performance statistics once optimal portfolio weights $\boldsymbol{w}_t^*$ and realized asset returns $\tilde{\boldsymbol{r}}_t$ have been calculated for all time-stamps $L + 1, \ldots, T$ where T is the maximum possible time-stamp.

4.1.2 Comparing portfolio returns against benchmarks

We perform the backtests for the 2-threshold Gerber covariance matrix and compare against benchmarks of using historical covariance matrix and 1-threshold Gerber covariance matrix. For these backtests, we fix the re-balancing frequency to monthly and set transaction cost term $\psi = 0.001$. Portfolio variance targets of 0.05, 0.1, 0.15, 0.2, 0.25, 0.3, 0.35 and 0.4 are tested to produce the efficient frontiers. Results are also compared across varying lookback periods L such as 6, 9, 12 time-stamps. In this section, we display the results for the backtest with lookback period $L = 6$ as it performed the best. For 1-threshold Gerber correlation common thresholds of $H = 0.5$ were used for all assets, and for 2-threshold Gerber correlation parameters were set as $P = 0.5$, $Q = 1$ and $\alpha = 0.5$. For other sensible choices of H, P, Q and α similar results were obtained in that the 2-threshold Gerber covariance estimation method consistently outperformed others for most parameter settings.

FIGURE 4.1: Backtest performance of the three covariance estimation methods in terms of annualized portfolio target variance and annualized return, given $H = 0.5$ for 1-threshold Gerber covariance and $P = 0.5$, $Q = 1$ and $\alpha = 0.5$ for 2-threshold Gerber covariance. $L = 6$ for all portfolios. **Green**: Performance of 2-threshold Gerber covariance based portfolios. **Orange**: Performance of 1-threshold Gerber covariance based portfolios. **Blue**: Performance of historical covariance based portfolios.
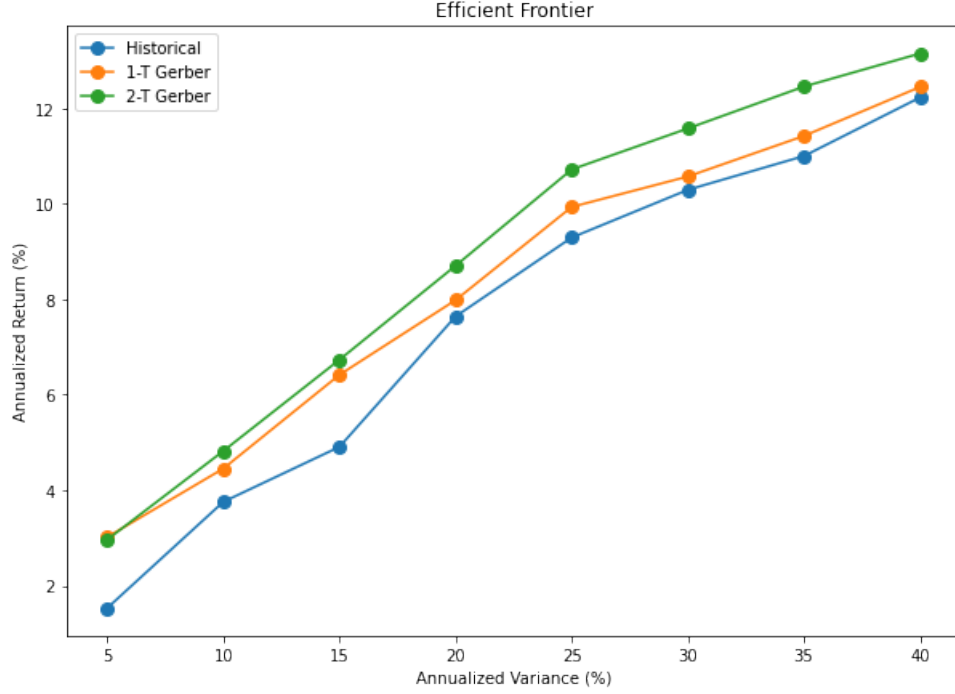
Figure 4.1 illustrates the efficient frontiers produced by the three covariance estimation methods under annualized target portfolio variance settings of 0.05, 0.1, 0.15, 0.2, 0.25, 0.3, 0.35 and 0.4. We see that the 2-threshold Gerber covariance based portfolios significantly outperform historical covariance based portfolios for all target variances considered. It also only marginally underperforms against the 1-threshold Gerber covariance based portfolio for target variance of 0.05 (5%) and outperforms for all other target variances. This illustrates superior portfolio performance of using 2-threshold Gerber covariance compared to the two benchmarks for the 10-year period between 2012 and 2022.

Key backtest statistics like annualized returns, cumulative returns, Sharpe Ratio and 95% VaR are displayed in Table 4.1. Sharpe ratio is defined as the annualized mean returns divided by annualized standard deviation of returns. It assesses risk-adjusted performance of a strategy and is a common metric to measure portfolio performance. Value at Risk (VaR) is a risk metric estimating the highest potential loss a portfolio

might experience over a given time frame, with a 95% VaR indicating the portfolio's return value for which there is 95% confidence in achieving better results.

We see that the 2-threshold Gerber covariance estimation method outperforms both the historical and 1-threshold Gerber covariance methods in terms of annualized returns, cumulative returns and Sharpe Ratio for almost all levels of target annualized variance. The 95% VaR tends to be marginally larger (in magnitude) than those for historical and 1-threshold Gerber covariance. These results suggest that using 2-threshold Gerber covariance leads to the distribution of portfolio returns to be slightly more risky, however both absolute and risk-adjusted returns metrics significantly outperform the benchmarks and hence the marginally increased risk is well-justified.

Figure C.1 in Appendix C show plots of cumulative portfolio returns for the three covariance matrix types across varying portfolio variance targets and lookback periods of 6, 9 and 12 months. Cumulative portfolio return plots further reveal that using Gerber covariance matrices in general lead to better performance during extreme market turbulence during 2020-2022 (COVID) compared to the historical covariance matrix. Moreover, the returns yielded using 2-threshold Gerber covariance outperform those yielded using 1-threshold Gerber covariance in most target variance-lookback combinations. This adds further evidence of outperformance of 2-threshold Gerber covariance against the two benchmarks.

4.1.3 Effect of parameters of 2-threshold Gerber correlation

We systematically vary parameter settings of 2-threshold Gerber correlation such as α, and P and Q to better understand the effect of these parameters on portfolio performance.

4.1.3.1 Varying weight α

With fixed parameter values of $P = 0.5$, $Q = 1$ and $\psi = 0.001$ and with varying lookback periods L of 6, 9, 12, 18 and 24 months, we explore how changes in α affect portfolio returns. As illustrated in Figure 2.2, α controls the co-movement weight given to partially concordant and discordant pairs with the weight assigning function $m_{ij}(t)$.

TABLE 4.1: Backtest performance metrics for historical covariance, 1-threshold Gerber covariance and 2-threshold Gerber covariance based portfolios at eight different risk target levels for the period between January 2012 and December 2022. Parameters were set as $H = 0.5$ for 1-threshold Gerber covariance and $P = 0.5$, $Q = 1$ and $\alpha = 0.5$ for 2-threshold Gerber covariance. $L = 6$ for all portfolios.

Target variance	Metrics	Historical	1-T Gerber	2-T Gerber
5 %	Annual Returns (%)	1.53	3.02	2.96
	Cumulative Returns (%)	117.14	136.30	135.54
	Sharpe Ratio	0.21	0.36	0.35
	95 % VaR (%)	−4.28	−4.21	−4.32
10 %	Annual Returns (%)	3.76	4.45	4.82
	Cumulative Returns (%)	146.82	157.41	163.29
	Sharpe Ratio	0.34	0.38	0.40
	95 % VaR (%)	−6.16	−6.13	−6.25
15 %	Annual Returns (%)	4.91	6.42	6.73
	Cumulative Returns (%)	164.70	191.13	197.12
	Sharpe Ratio	0.36	0.44	0.45
	95 % VaR (%)	−7.72	−7.67	−7.81
20 %	Annual Returns (%)	7.64	7.98	8.70
	Cumulative Returns (%)	215.29	222.52	238.48
	Sharpe Ratio	0.45	0.47	0.49
	95 % VaR (%)	−9.15	−9.18	−9.26
25 %	Annual Returns (%)	9.29	9.93	10.72
	Cumulative Returns (%)	252.31	268.16	288.80
	Sharpe Ratio	0.48	0.50	0.53
	95 % VaR (%)	−10.64	−10.55	−10.72
30 %	Annual Returns (%)	10.29	10.57	11.58
	Cumulative Returns (%)	277.42	284.82	313.01
	Sharpe Ratio	0.49	0.50	0.53
	95 % VaR (%)	−11.49	−11.50	−11.72
35 %	Annual Returns (%)	11.00	11.42	12.45
	Cumulative Returns (%)	296.52	308.47	339.62
	Sharpe Ratio	0.51	0.52	0.54
	95 % VaR (%)	−11.94	−11.97	−12.28
40 %	Annual Returns (%)	12.23	12.45	13.15
	Cumulative Returns (%)	332.51	339.38	362.09
	Sharpe Ratio	0.54	0.54	0.55
	95 % VaR (%)	−12.31	−12.42	−12.75

FIGURE 4.2: Box plot of annualized portfolio returns against target annualized portfolio variance obtained with varying lookback periods, grouped by α values.
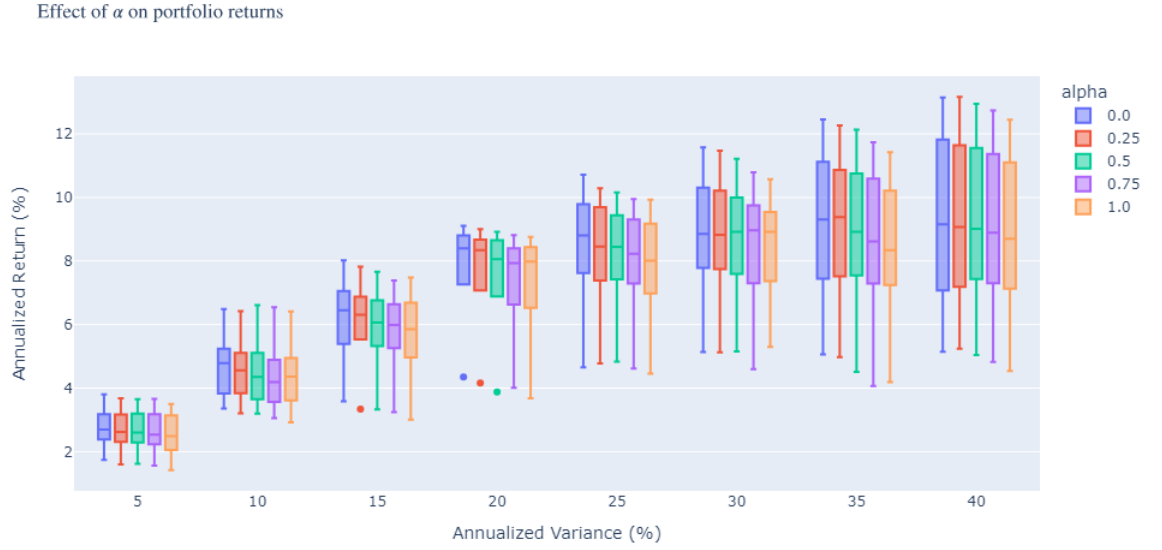
α values of 0, 0.25, 0.5, 0.75 and 1 are tested. For each chosen α, five backtests are run (for the five different lookback periods) following steps described in 4.1.1.

Results are shown as a boxplot in Figure 4.2 where each box summarizes five portfolio returns (for five different lookback periods) obtained under chosen target annualized variance and α settings. We see a common pattern across the annualized variance values on the x-axis that higher portfolio returns are obtained when the value of α is lower, in general. This suggests that better portfolio performance is achieved when we completely silence the co-movement weight of partially concordant and discordant pairs as opposed to giving them some positive weight. Note the 2-threshold Gerber correlation with $\alpha = 0$ is still different to the original 1-threshold Gerber correlation as it defines extra off-diagonal regions with co-movement weight of 0 compared to the 1-threshold Gerber correlation.

4.1.3.2 Horizontal shift of P and Q

With fixed parameter values of $\alpha = 0$ and $\psi = 0.001$ and with varying lookback periods L of 6, 9, 12, 18 and 24 months, we explore how changes in the location of (P, Q) affect portfolio returns. We fix the width as 1 (i.e., $Q - P = 1$) and test $(0, 1)$, $(0.25, 1.25)$,

FIGURE 4.3: Box plot of annualized portfolio returns against target annualized portfolio variance obtained with varying lookback periods, grouped by (P, Q) values.
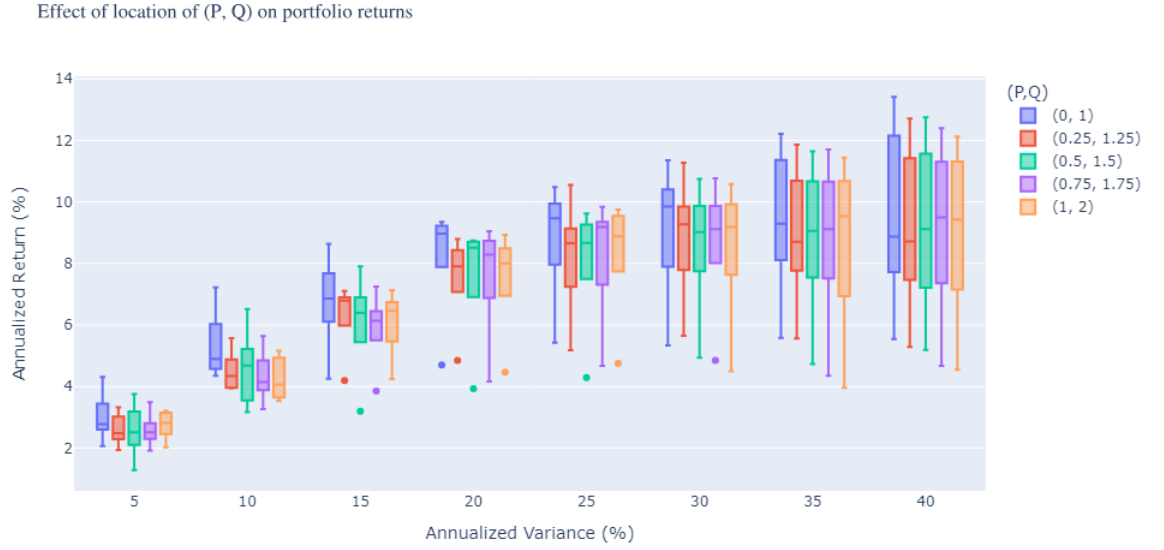
(0.5, 1.5), (0.75, 1.75), (1, 2) as values of (P, Q). For each (P, Q) pair, five backtests are run (for the five different lookback periods) following steps described in 4.1.1.

In Figure 4.3 we see that $(P, Q) = (0, 1)$ consistently yields the best portfolio performance across various target variance levels. It consistently has the highest upper quartile portfolio returns as well generally higher maximum, median, lower quartile, and minimum portfolio returns compared to other pairs of (P, Q) tested. This result suggests that we can achieve higher portfolio returns when we do not completely discard pairs of returns observations with small magnitudes as *noise* but actually give some weight according to $m_{ij}(t)$.

4.1.3.3   Effect of Q

With fixed parameter values of $\alpha = 0$, $\psi = 0.001$, $P = 0$ and with varying lookback periods L of 6, 9, 12, 18 and 24 months, we explore how changes in the larger threshold Q affect portfolio returns. We test $0.25, 0.5, 0.75, 1, 2$ as possible values of Q. For each chosen Q, five backtests are run (for the five different lookback periods) following steps described in 4.1.1.

FIGURE 4.4: Box plot of annualized portfolio returns against target annualized portfolio variance obtained with varying lookback periods, grouped by Q values.
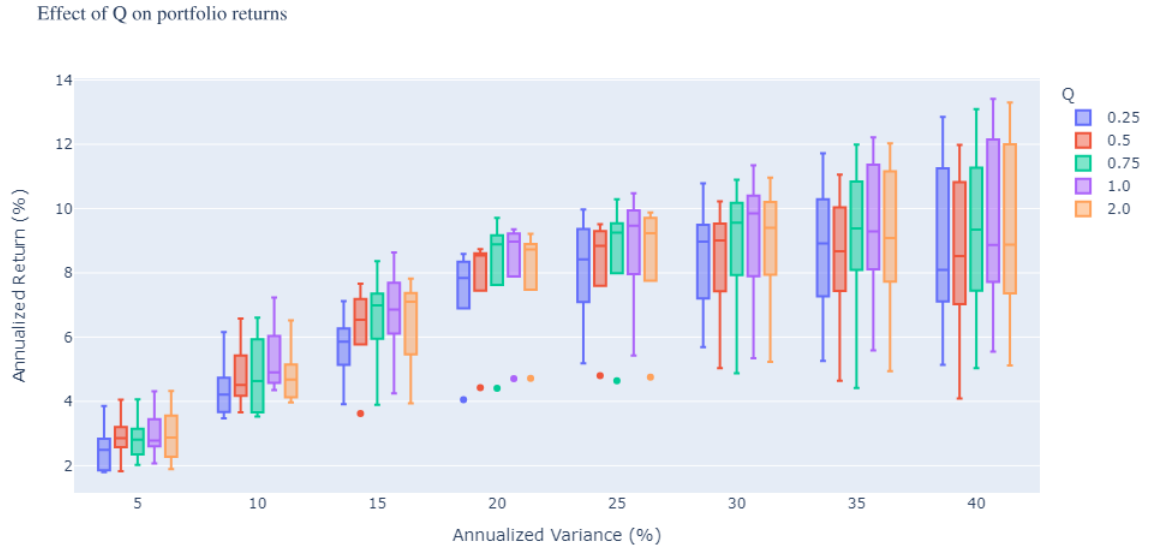
Figure 4.4 shows the results. Patterns in the effect of Q are less observable than other tests conducted above. Under low volatility constraints such as target portfolio variances of 5% and 10% especially, there exists little difference in the distribution of portfolio returns between different choices of Q. If anything, we see $Q = 1$ tends to consistently yield the best results across multiple target variance levels. Overall, the relative insensitivity of portfolio returns to Q suggests the threshold used to decide whether data exceeding it is deemed outliers and given flat co-movement weight of 1 does not have overly significant effect on the performance of 2-threshold Gerber covariance based portfolios, although $Q = 1$ does result in marginally better backtest results overall.

4.2 Twenty-two assets

We perform similar kind of analysis presented in 4.1 with a larger universe of assets for the period between June 2015 and December 2022. From the list of stocks of S&P500 as at July 2023 we randomly pick 2 stocks each from a total of 11 sectors to form a universe of 22 sector-diversified US stocks (see Table C.1 in Appendix C for the list of 22 stocks selected). Backtests are performed following the steps described in 4.1.1.

Figure 4.5 shows the efficient frontiers obtained using 2-threshold Gerber, 1-threshold Gerber and historical covariance matrices. We observe that across all lookback periods, the performance of 2-threshold Gerber covariance based portfolios in general outperform the other two, for most target anunalized variance levels. For shorter lookback periods such as $L = 6$ and 9 months, underperformance of 2-threshold Gerber covariance method under low portfolio variance conditions is more noticeable. Nevertheless, outperforming the benchmarks for most lookback periods and target variance levels add support for the superior performance and robustness of 2-threshold Gerber covariance based portfolios.

Figure C.2 in Appendix C shows a box plot of annualized portfolio returns against target variance levels obtained with varying look back periods of 6, 9, 12, 18 and 24 months, grouped by α values. Fixed parameter values of $P = 0.5$, $Q = 1$ and $\psi = 0.001$ are used. Similarly to the results for nine assets as shown in section 4.1.3.1, lower α values tend to outperform for most target variance levels. Except for very low-volatility target variance levels of 5% and 10%, this trend is easily visible. This adds supporting evidence that lower α values are more performant and robust across different data sets.

With fixed parameter values of $\alpha = 0$, $\psi = 0.001$ and lookback periods L of 6, 9, 12, 18 and 24 months, we vary (P, Q) to be $(0, 1), (0.25, 1.25), (0.5, 1.5), (0.75, 1.75), (1, 2)$. Figure C.3 shows the results. Unlike the results illustrated in section 4.1.3.2 for the nine asset universe, there is less of an observable pattern in which a certain choice of (P, Q) uniformly outperforms the others. This suggests that the choice of (P, Q) may be more dependent on the data itself and that there is less chance of a true pattern existing.

With fixed parameter values of $P = 0$, $\alpha = 0$, $\psi = 0.001$ and lookback periods L of 6, 9, 12, 18 and 24 months, we vary Q to be $0.25, 0.5, 0.75, 1, 2$. Figure C.4 shows the results. Like the results illustrated in section 4.1.3.3 for the nine asset universe, there is not a strongly observable pattern in the effect of Q across various target variance levels. Again, for moderate and larger variance levels such as greater than 10%, $Q = 1$ does seem to have higher maximum, median and minimum portfolio returns in general.

FIGURE 4.5: Backtest performances on the 22 US stocks universe, with varying look-back periods L. Other parameters fixed as $H = 0.5$, $P = 0.5$, $Q = 1$ and $\alpha = 0.5$. **Green**: Performance of 2-threshold Gerber covariance based portfolios. **Orange**: Performance of 1-threshold Gerber covariance based portfolios. **Blue**: Performance of historical covariance based portfolios.
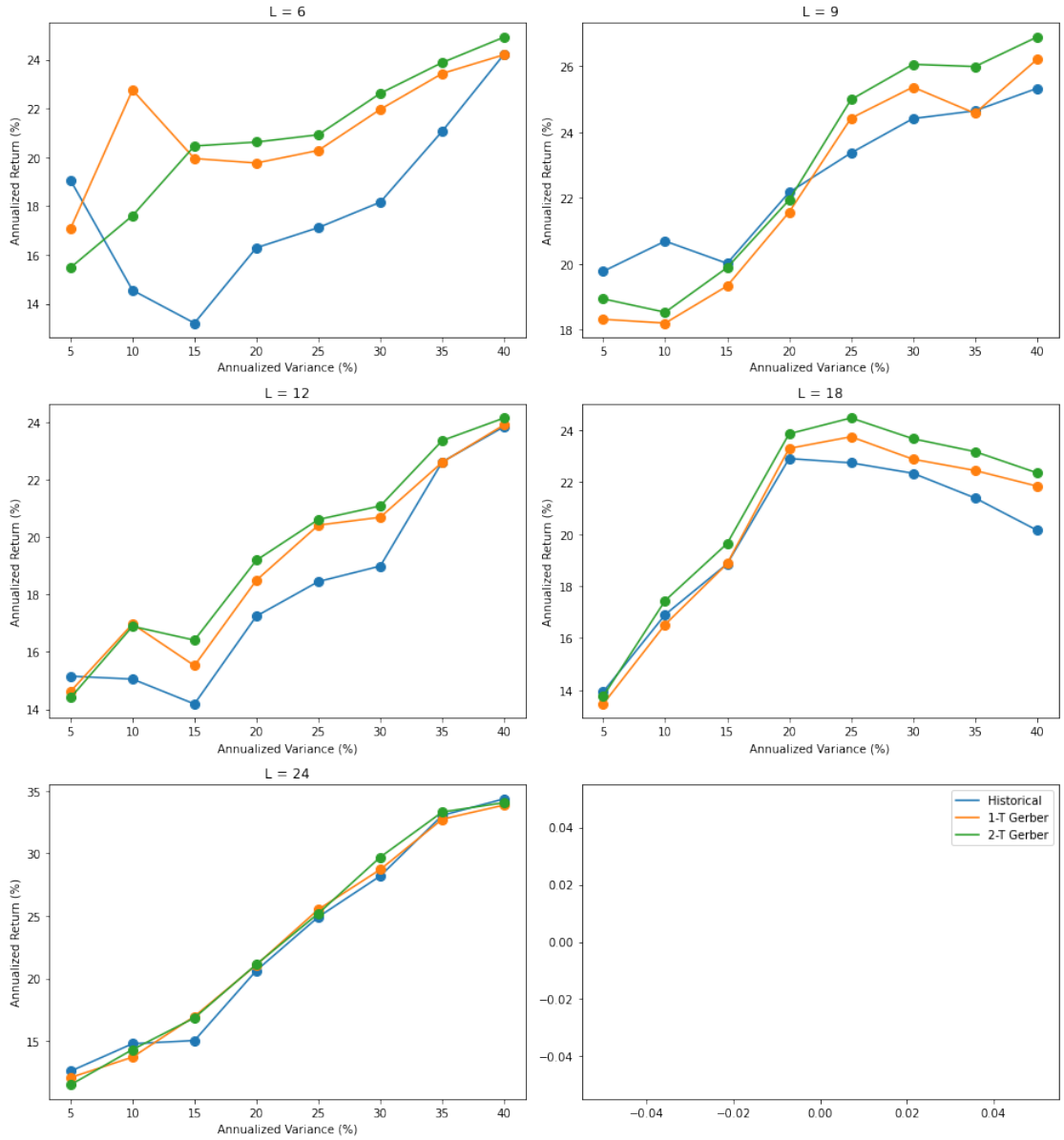
Chapter 5

Time-varying Gerber correlation

In modern portfolio optimization, the accurate measurement of asset interdependence plays a pivotal role in constructing robust and efficient portfolios. Correlation and covariance measures such as Pearson's, Kendall's Tau and Gerber are employed to assess the relationship between assets, assuming a constant level of dependence over time (i.e., each data point contributes equally to the estimate disregarding recency). However, this assumption overlooks the evolving nature of financial markets, where correlations may exhibit temporal fluctuations due to changing market dynamics and evolving economic conditions.

In this chapter we extend the n-threshold Gerber correlation by incorporating the Exponentially Weighted Moving Average (EWMA) method (Hunter, 1986). This integration allows for the consideration of dynamic dependence contributions based on the recency of data points, thereby providing a more market-adaptive and relevant correlation measure. By granting greater weight to recent data, the proposed time-varying Gerber correlation seeks to address the limitations of fixed-dependence models and be more responsive to ever-changing dynamics of financial markets.

In the subsequent sections of this chapter, we will delve into the theoretical framework of the proposed time-varying Gerber correlation with the EWMA method. We present the mathematical formulations, discuss the advantages of incorporating dynamic dependence contributions, and illustrate the significance of considering recent data points

in correlation calculations. Furthermore, we conduct empirical analyses using historical financial data to demonstrate the practical implications of our method in portfolio optimization scenarios.

5.1 Exponentially Weighted Moving Average

The exponentially weighted moving average (EWMA) is a weighted average statistic that assigns exponentially decaying weight to data points as they get older. It is a popular type of time-series smoothing method used by practitioners in finance. With an appropriate choice of the decay parameter λ, one can perform an appropriate smoothing transformation of the original returns time-series data in the form of weighted moving average that is more reactive to recent data.

In this section, we briefly introduce how the EWMA method is applied to a time-series data such as asset returns and describe the effect of λ. While there are a few kinds of EWMA methods that are often referred to, we adopt the formulation described by Hunter (1986). We extend the n-threshold Gerber correlation statistic using the EWMA method and develop the time-varying EWMA Gerber correlation statistic.

The recursive form of EWMA of time-series data $(x_1, \ldots, x_T)$ at time-stamp t where $t = 1, \ldots, T$ can defined as

$$\hat{x}_t = \begin{cases} x_1 & t = 1 \\ \lambda x_t + (1 - \lambda)\hat{x}_{t-1} & t > 1, \end{cases} \tag{5.1}$$

where $\hat{x}_t$ is the EWMA value at time t and $0 \leq \lambda \leq 1$ is the decay parameter that determines the sensitivity of the EWMA to recent data (i.e., how quick the weight for past information decays). The higher the λ the less smooth the resulting EWMA time-series will be as it is more responsive to the most recent data point x_t.

Hunter (1986) shows we can re-write $\hat{x}_t$ as

$$\hat{x}_{t+1} = \sum_{t=0}^{T} w_t x_t \tag{5.2}$$

where $w_t = \lambda(1-\lambda)^{t-1}$. This formulation gives rise to the name Exponentially Weighted Moving Average as the weight of preceding data point is multiplied by $(1-\lambda)$ for each t. Figure 5.1 illustrates three sequences of exponentially decaying weights through time for $t = 1, \ldots, 50$, obtained with $\lambda = 0.1, 0.3, 0.5$.

FIGURE 5.1: EWMA weight w_t for each t for $\lambda = 0.1, 0.3, 0.5$.
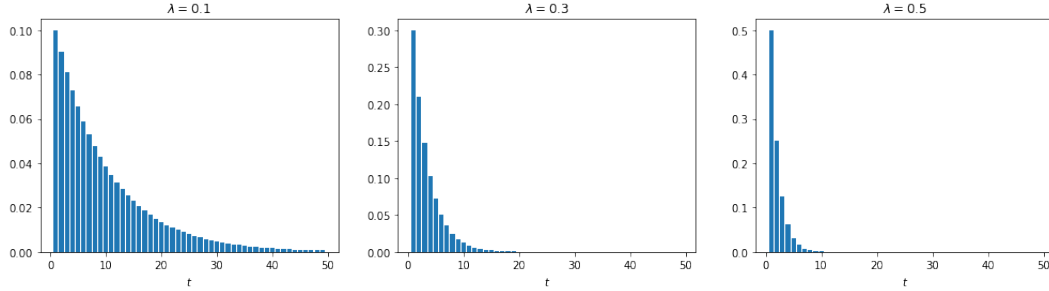
Figure 5.2 illustrates a white noise time-series observation $(x_1, \ldots, x_{150})$ in blue and three EWMAs applied on it with $\lambda = 0.1, 0.3, 0.5$ for example.

FIGURE 5.2: Three EWMAs computed on white noise observations $(x_1, \ldots, x_{150})$ with varying decay parameter λ.
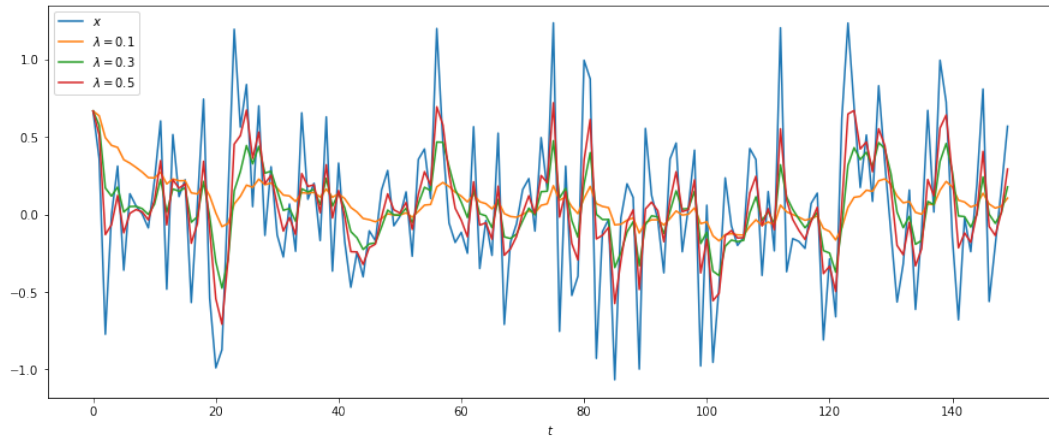
5.2 EWMA Gerber correlation

In this section we develop an extension of Gerber correlation statistic by incorporating the EWMA method that computes the correlation values while assigning exponentially decaying weights to older data. Using the EWMA Gerber correlation eliminates the need for setting a specific lookback period L to base calculation of correlations on by introducing the decay parameter λ that is more intuitive to understand.

Recall the n-threshold Gerber correlation matrix $\boldsymbol{G}$ consisting of entries

$$g_{ij} = \frac{\sum_{t=1}^{T} m_{ij}(t)}{T - n_{ij}^{NN}} \tag{5.3}$$

where the weighting function $m_{ij}(t)$ characterizes the n-threshold Gerber correlation for a specific $n \geq 1$ and is defined as in equation 2.9.

We first decompose n_{ij}^{NN} into a t-specific function $n_{ij}^{NN}(t)$ where $n_{ij}^{NN} = \sum_{i=1}^{T} n_{ij}^{NN}(t)$. For n-threshold Gerber correlation with $m_{ij}(t)$ as defined in equation 2.9 we have $n_{ij}^{NN}(t) := |\{(i,j) \ : \ |r_{ti}| < C_1, \ |r_{tj}| < C_1\}|$. This decomposition allows us to write both the numerator and denominator of g_{ij} as functions of data from a certain start period ($t = 1$ here) to the end period ($t = T$ here) as

$$g_{ij} = \frac{\sum_{t=1}^{T} m_{ij}(t)}{\sum_{t=1}^{T} \left[1 - n_{ij}^{NN}(t)\right]}, \tag{5.4}$$

where we can now vary the start and end periods depending on the exact time-stamps we want the Gerber correlation statistic to be based on.

Now, define $\tilde{\boldsymbol{G}}(t)$, the time t-specific Gerber correlation matrix that depends only on the observations at time t or on the past q_t observations where q_t is minimal such that $\sum_{s=t-q_t}^{t} \left[1 - n_{ij}^{NN}(s)\right] \neq 0$. Using equation 5.4 and desired start and end periods, $\tilde{\boldsymbol{G}}(t)$ has entries $\tilde{g}_{ij}(t)$ such that

$$\tilde{g}_{ij}(t) = \begin{cases} \frac{m_{ij}(t)}{1 - n_{ij}^{NN}(t)} & \text{if } n_{ij}^{NN}(t) \neq 1 \\ \frac{\sum_{s=t-q_t}^{t} m_{ij}(s)}{\sum_{s=t-q_t}^{t} \left[1 - n_{ij}^{NN}(s)\right]} & \text{otherwise.} \end{cases} \tag{5.5}$$

$\tilde{\boldsymbol{G}}(t)$ will play the same role as x_t in equation 5.1. It represents the most granular and recent unit of valid Gerber correlation matrix in the EWMA formulation.

We define the EWMA Gerber correlation matrix $\hat{\boldsymbol{G}}(t)$ for time-stamps $t = R, \dots, T$ as

$$\hat{\boldsymbol{G}}(t) = \begin{cases} \left[\frac{\sum_{s=1}^{R} m_{ij}(s)}{\sum_{s=1}^{R} \left[1 - n_{ij}^{NN}(s)\right]}\right]_{i=1, j=1}^{K, \ K} & t = R \\ \lambda \tilde{\boldsymbol{G}}(t) + (1 - \lambda) \hat{\boldsymbol{G}}(t - 1) & t > R. \end{cases} \tag{5.6}$$

Here, $R \geq 1$ is the smallest possible integer *ramp-up period* that makes $\sum_{s=1}^{R} \left[1 - n_{ij}^{NN}(s)\right] \neq 0$ for all pairs of assets (i,j). The decay parameter $0 \leq \lambda \leq 1$ is used to determine the

sensitivity of EWMA to recent data. We observe empirically that $\lambda < 0.1$ usually leads to better results.

Applying the EWMA method to n-threshold Gerber correlation matrix directly on the correlation matrix like above preserves positive semi-definiteness given that the n-threshold Gerber correlation in question is positive semi-definite (under appropriate conditions where necessary). Positive semi-definiteness of $\hat{\boldsymbol{G}}(t)$ in equation 5.6 is proved in Appendix D.1.

The asset allocation problem 1.2 requires a valid covariance matrix as input. For this, we use the EWMA Gerber covariance matrix defined as

$$\hat{\boldsymbol{\Sigma}}(t) = \text{diag}(\boldsymbol{\sigma}(t)) \, \hat{\boldsymbol{G}}(t) \, \text{diag}(\boldsymbol{\sigma}(t)) \tag{5.7}$$

where $\boldsymbol{\sigma}(t)$ is a K $\times$ 1 vector of sample standard deviations of the set of historical asset returns observed at time t.

Figure 5.3 illustrate the 1-threshold EWMA Gerber correlation between stock returns of META (Meta Platforms, or Facebook) and AMZN (Amazon) between January 2022 and January 2023. Decay parameters of $\lambda = 0.01, 0.05, 0.1$ are shown as examples. We can see higher λ of 0.1 yields more reactive and sensitive EWMA correlation time-series and lower λ of 0.01 yields steadier and more persistent EWMA correlation time-series. What kind of λ is preferred would be data-dependent and need to be backtested.

FIGURE 5.3: 1-threhsold EWMA Gerber correlations on stock returns of META and AMZN between Jan. 2022 and Jan. 2023 for $\lambda = 0.01, 0.05, 0.1$.
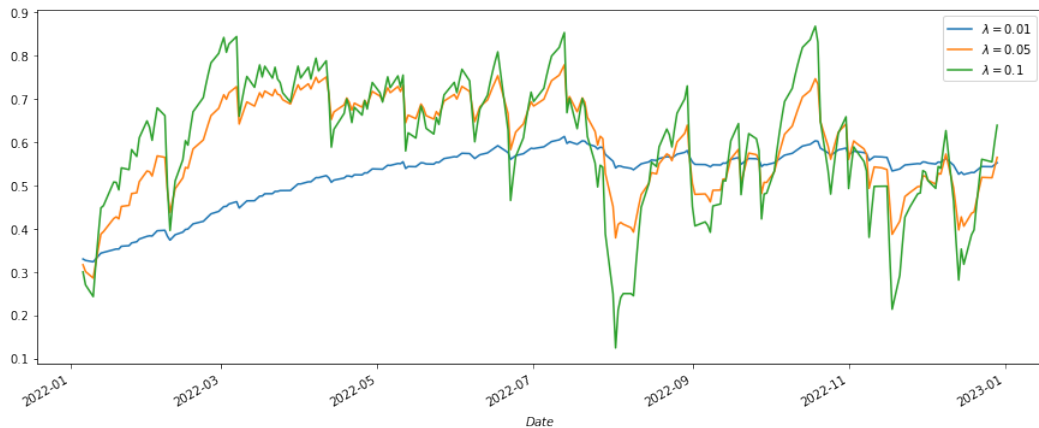
5.3 Empirical Study

5.3.1 Backtesting procedure

Backtesting procedure for asset allocation using n-threshold EWMA Gerber covariance matrix is described as follows:

1. Set re-balancing frequency (e.g., monthly), lookback window L for the estimation of the expected returns $\boldsymbol{\mu}$, and decay parameter λ for EWMA correlation calculation.

2. Set the values of other parameters like the transaction cost term ψ, portfolio variance target σ_{target}^2, and Gerber-specific parameters like number of thresholds n and related values such as thresholds and partial co-movement weights.

3. Asset returns data, at chosen re-balancing frequency, are retrieved for the period January 2012 to December 2022. Returns are calculated as percentage differences, $r_{t,i} = \frac{price_t}{price_{t-1,i}} - 1$.

4. Returns data of K assets for the first L time-stamps, i.e., $\boldsymbol{r}_t := (r_{t1}, \ldots, r_{tK})$ for $t = 1, \ldots, L$ are then standardized with $\hat{\boldsymbol{r}}_t := (\hat{r}_{t1}, \ldots, \hat{r}_{tK})$ where $\hat{r}_{tk} = \frac{r_{tk} - \bar{r}_k(t)}{\sigma_k(t)}$, which is used to compute $\boldsymbol{\mu} = \frac{1}{L} \sum_{t=1}^{t=L} \hat{\boldsymbol{r}}_t$ and EWMA Gerber covariance matrix $\hat{\boldsymbol{\Sigma}}$ using equation 5.7.

5. Solve the convex optimization problem 1.2 by substituting $\boldsymbol{\mu}$ and $\boldsymbol{\Sigma}$ and find the optimal portfolio weight for the next time-stamp $\boldsymbol{w}_{L+1}^*$ given maximum allowed portfolio variance σ_{target}^2.

6. Re-balance the portfolio according to $\boldsymbol{w}_{L+1}^*$ and hold it for next unit of time-stamp. At the end of the holding period, calculate portfolio returns with $\boldsymbol{w}_{L+1}^{*T} \tilde{\boldsymbol{r}}_{L+1}$ where $\tilde{\boldsymbol{r}}_{L+1}$ is the realized asset returns for the time-stamp $L+1$.

7. Repeat steps 4 to 6 by shifting the lookback period one time-stamp forward each time.

8. Compute various portfolio performance statistics once optimal portfolio weights $\boldsymbol{w}_t^*$ and realized asset returns $\tilde{\boldsymbol{r}}_t$ have been calculated for all time-stamps $L+1, \ldots, T$ where T is the maximum possible time-stamp.

Above backtesting procedure for EWMA method is very similar to the standard procedure shown in 4.1.1. Key difference is that with EWMA we use the decay parameter λ to calculate EWMA Gerber covariance matrix instead of relying on the lookback window L to calculate the Gerber covariance matrix on in a moving window. Note the lookback window L is still used in 5.3.1 to calculate the expected returns $\boldsymbol{\mu}$ at each time-stamp. Our goal is to sorely investigate the effect of using EWMA Gerber covariance matrix compared to the standard Gerber covariance matrix.

5.3.2 Nine assets

We first backtest a range of λ values for 1-threshold EWMA covariance matrix based portfolio optimization using the nine assets described in 4.1. We fix the re-balancing frequency to monthly and set transaction cost term $\phi = 0.001$. Portfolio variance targets of $0.05, 0.1, 0.15, 0.2, 0.25, 0.3, 0.35, 0.4$ and lookback periods $6, 9, 12, 18, 24$ are tested with $\lambda = 0.01, 0.025, 0.05, 0.075, 0.1, 0.2, 0.3$. We explore how changes in decay parameter λ affect portfolio returns.

Results are shown as a boxplot in Figure D.1 where each box summarizes five portfolio returns (for five different lookback periods) obtained under chosen target annualized variance and λ. The Figure illustrates that $\lambda = 0.01$ which is the smallest decay parameter value considered, outperforms others in most target portfolio variance settings.

Figure 5.4 illustrates the efficient frontiers obtained using 1-threshold Gerber and 1-threshold EWMA Gerber covariance matrices with fixed decay parameter $\lambda = 0.01$. We observe that the 1-threshold EWMA Gerber covariance based portfolios outperform across all target portfolio variance levels for lookback window $L = 12$ but tend to underperform for longer lookback windows $L = 18, 24$. For shorter lookback windows, it performs comparably to the non-EWMA counterpart. This shows applying EWMA on 1-threshold Gerber covariance can indeed improve portfolio performance in certain situations but not always. This discovery underscores the potential value of the EWMA 1-threshold Gerber covariance as a viable alternative when it comes to selecting an estimation method for covariance matrix.

FIGURE 5.4: Backtest performances on the 9-asset universe, with varying lookback periods L for fixed decay parameter $\lambda = 0.01$. **Orange:** Performance of 1-threshold EWMA Gerber covariance based portfolios. **Blue:** Performance of 1-threshold Gerber covariance based portfolios.
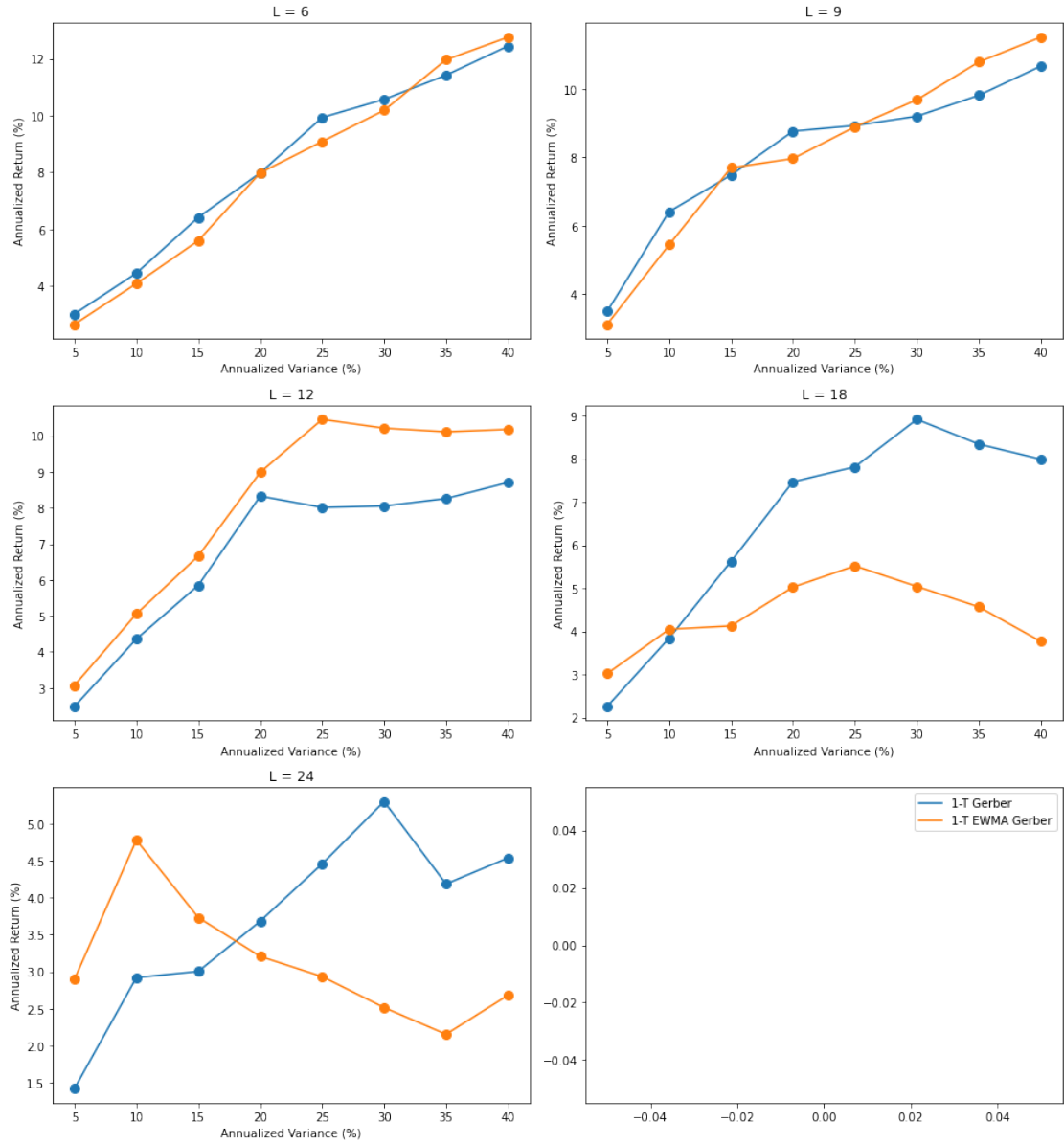
5.3.3 Twenty-two assets

We backtest the 1-threshold EWMA Gerber covariance based portfolios on the 22 US stocks universe introduced in section 4.2. We fix the re-balancing frequency to monthly and set transaction cost term $\phi = 0.001$. Portfolio variance targets of 0.05, 0.1, 0.15, 0.2, 0.25, 0.3, 0.35, 0.4 and lookback periods $6, 9, 12, 18, 24$ are tested with $\lambda = 0.01, 0.025, 0.05, 0.075, 0.1, 0.2, 0.3$. Results are shown as a boxplot in Figure D.2 where each box summarizes five portfolio returns (for five different lookback periods) obtained under chosen target annualized variance and λ. The Figure illustrates that there is no one λ value that outperforms in all target variance settings. $\lambda = 0.05$ out of all seems to have generally good returns and consistency (suggested by not exceedingly long box sizes) across most target variance settings.

Figure D.3 illustrates the efficient frontiers obtained using 1-threshold Gerber and 1-threshold EWMA Gerber covariance matrices with fixed decay parameter $\lambda = 0.05$. In parallel with the findings within the context of the 9-asset universe, it is evident that the portfolio constructed using the 1-threshold EWMA Gerber covariance does not consistently exhibit superior performance when compared to its non-EWMA counterpart. Nevertheless, a discernible improvement in portfolio performance is observed under specific conditions. This enhancement becomes pronounced when considering portfolios with moderately high variance targets exceeding 10% for values of $L = 6, 12$.

5.3.4 2-threshold EWMA Gerber covariance portfolios

We also conducted backtests for 2-threshold EWMA Gerber covariance portfolios on the two asset universes, and our findings exhibited similar trends as observed in Figures D.4 and D.5. Employing the EWMA method yielded enhancements compared to its non-EWMA counterpart under specific conditions; however, these improvements were not universally applicable across all parameter settings.

Chapter 6

Conclusion

Chapter 1 introduced the asset allocation problem within the context of Mean-Variance Portfolio optimization. Emphasis was placed on the critical role of accurate models for forecasting portfolio risk, notably characterized by the co-movements among assets in a portfolio. Common measures of correlations, such as Pearson's correlation coefficient, widely used in practice to address the Mean-Variance Portfolio optimization problem, were discussed, alongside their associated limitations when applied to financial data.

Chapter 2 provided a review of the 1-threshold Gerber correlation statistic (Gerber et al., 2022), which aimed to address the aforementioned limitations by offering a more robust representation of asset co-movements. Building upon this foundation, we developed the n-threshold Gerber correlation statistic, affording finer granularity in the characterization of varying co-movement strengths, particularly within the tails. Additionally, we derived the sufficient conditions for ensuring the positive semi-definiteness of an n-threshold Gerber correlation matrix, thereby establishing its validity as a correlation matrix for describing asset co-movements. In particular, for the 2- and 3-threshold Gerber correlation statistics, we derived a more generalized set of sufficient conditions that expanded the feasible region for partial co-movement weights. To further enhance flexibility, we developed the tanh-tanh Gerber correlation statistic, which aimed to assign co-movement weights in a continuous fashion.

Chapter 3 delved into a comprehensive simulation study aimed at empirically validating the positive semi-definiteness of 1-, 2-, and 3-threshold Gerber correlation matrices. This

investigation confirmed the positive semi-definiteness of these Gerber correlation matrices. Furthermore, we explored the positive semi-definiteness of the tanh-tanh Gerber correlation matrix and identified instances where it did not meet this criterion, rendering it unsuitable as a valid correlation measure for now.

Chapter 4 featured an extensive empirical study comparing portfolio performance constructed using the 2-threshold Gerber correlation matrix as an input for risk in MVP optimization problems with those constructed using Pearson's and 1-threshold Gerber correlation. For both well-diversified asset universes considered, portfolios based on the 2-threshold Gerber correlation matrix consistently outperformed their counterparts in most scenarios, underscoring the advantages gained by our ability to more flexibly model the degree of co-movements in the tail regions.

Finally, in Chapter 5, we introduced the EWMA Gerber correlation statistic, which takes into account the dynamic dependence contributions of past data points based on their recency. This approach yielded a more market-adaptive and contextually relevant Gerber correlation measure, removing the need for specifying a fixed lookback period L that was previously employed to artificially derive time-varying correlation measures for portfolio construction. We established the conditions for positive semi-definiteness of n-threshold EWMA Gerber correlation matrices and conducted empirical tests of portfolio performance. The results revealed that portfolios constructed using n-threshold EWMA Gerber correlation matrices sometimes outperformed their non-EWMA counterparts, indicating the potential utility of the n-threshold EWMA Gerber correlation statistic as an additional tool in the arsenal of financial practitioners.

6.1 Future work

Due to time limitations, we have derived a set of relatively strict sufficient conditions for positive semi-definiteness of arbitrary n-threshold Gerber correlation statistic, along with slightly more general sufficient conditions applicable to the 2- and 3-threshold Gerber correlation statistics. An important avenue for enhancing the utility of Gerber correlation statistics lies in our quest to formulate both necessary and sufficient conditions for positive semi-definiteness of the correlation matrix in terms of the co-movement weights $\{\alpha_i\}_{i=2}^n$.

Furthermore, we have conceptualized another novel correlation measure termed the Ring correlation. In contrast to the Gerber correlation statistic, which assigns progressively increasing co-movement weights (in absolute value) to regions closer to the leading diagonals going through the origin (both in the positive and negative directions), the Ring correlation statistic assigns progressively decreasing co-movement weights to regions closer to the origin, with specific thresholds that define various concentric ring-like structures around the origin. The Ring correlation affords the capability to describe co-movement relationships pertaining to extreme events in asset return pairs, regardless of their directions. By formally defining the Ring correlation and potentially incorporating it with the n-threshold Gerber correlation statistic, we envision the development of a further extension of Gerber correlation. This extension would entail larger co-movement weights assigned to pairs of asset returns situated closer to the leading diagonals and further from the origin.

At present, we do not have a working version of continuous Gerber correlation statistic that ensures guaranteed positive semi-definiteness. While the tanh-tanh Gerber correlation statistic is a promising candidate, it needs further research and modification to meet the positive semi-definiteness criterion. Another research avenue involves exploring potential theoretical linkages between the n-threshold Gerber correlation statistic (possibly with the incorporation of Ring correlation as well) and the continuous Gerber correlation statistic that will be developed. Whether the continuous Gerber correlation statistic can be expressed as the limit of the n-threshold Gerber correlation statistic with $n \to \infty$ dependent upon a specific sequence of weights denoted as $\{\alpha_i\}_{i=2}^{n}$ is an interesting research question. Other choices of continuous functions may be considered in lieu of the tanh function, aimed at assigning co-movement weights that exhibit sensitivity to tail behaviors while mitigating the influence of noise associated with low-magnitude data points.

Appendix A

Appendix for Gerber correlation

A.1   2-threshold Gerber correlation

Positive semi-definiteness of 1-threshold Gerber correlation statistic has been proved in Gerber et al. (2023). We prove positive semi-definiteness of 2-threshold Gerber correlation statistic (equation 2.5) by adopting the approach presented in the paper.

Define new functions of r_{tk} and thresholds P and Q

$$f_{tk}^{(0)} = \begin{cases} 1 & \text{if } r_{tk} \geq P \\ -1 & \text{if } r_{tk} < -P \\ 0 & \text{otherwise} \end{cases} \tag{A.1}$$

$$f_{tk}^{(1)} = \begin{cases} 1 & \text{if } P \leq r_{tk} < Q \\ -1 & \text{if } -Q \leq r_{tk} < -P \\ 0 & \text{otherwise} \end{cases} \tag{A.2}$$

$$f_{tk}^{(2)} = \begin{cases} 1 & \text{if } r_{tk} \geq Q \\ -1 & \text{if } r_{tk} < -Q \\ 0 & \text{otherwise.} \end{cases} \tag{A.3}$$

Consider $T \times K$ sized matrices $\boldsymbol{F}^{(0)}$, $\boldsymbol{F}^{(1)}$ and $\boldsymbol{F}^{(2)}$ with entries $f_{tk}^{(0)}$, $f_{tk}^{(1)}$ and $f_{tk}^{(2)}$, respectively. Let $\langle \boldsymbol{F}_i, \boldsymbol{F}_j \rangle$ denote dot product of columns i and j of matrix $\boldsymbol{F}$ corresponding to assets i and j.

We express the numerator of g_{ij} (from equation 2.5) as

$$\sum_{i=1}^{T} m_{ij}(t) = \langle \boldsymbol{F}_i^{(1)}, \boldsymbol{F}_j^{(1)} \rangle + \langle \boldsymbol{F}_i^{(2)}, \boldsymbol{F}_j^{(2)} \rangle + \alpha(\langle \boldsymbol{F}_i^{(1)}, \boldsymbol{F}_j^{(2)} \rangle + \langle \boldsymbol{F}_i^{(2)}, \boldsymbol{F}_j^{(1)} \rangle). \tag{A.4}$$

We can then express the numerator matrix of 2-threshold Gerber correlation matrix $\boldsymbol{G}$ with entries g_{ij} as

$$\boldsymbol{G}_{NUM} := \boldsymbol{F}^{(1)T}\boldsymbol{F}^{(1)} + \boldsymbol{F}^{(2)T}\boldsymbol{F}^{(2)} + \alpha(\boldsymbol{F}^{(1)T}\boldsymbol{F}^{(2)} + \boldsymbol{F}^{(2)T}\boldsymbol{F}^{(1)}). \tag{A.5}$$

$\boldsymbol{G}_{NUM}$ is positive semi-definite when $\boldsymbol{x}^T\boldsymbol{G}_{NUM}\boldsymbol{x} \geq 0$ for any vector $\boldsymbol{x} \in \mathbb{R}^K$. Now,

$$\boldsymbol{x}^T\boldsymbol{G}_{NUM}\boldsymbol{x} = (\boldsymbol{F}^{(1)}\boldsymbol{x})^T(\boldsymbol{F}^{(1)}\boldsymbol{x}) + (\boldsymbol{F}^{(2)}\boldsymbol{x})^T(\boldsymbol{F}^{(2)}\boldsymbol{x}) + \alpha[(\boldsymbol{F}^{(1)}\boldsymbol{x})^T(\boldsymbol{F}^{(2)}\boldsymbol{x}) + (\boldsymbol{F}^{(2)}\boldsymbol{x})^T(\boldsymbol{F}^{(1)}\boldsymbol{x})].$$
$$\tag{A.6}$$

Denote $\boldsymbol{F}^{(1)}\boldsymbol{x} = (\beta_{11}, \ldots, \beta_{1K})^T$ and $\boldsymbol{F}^{(2)}\boldsymbol{x} = (\beta_{21}, \ldots, \beta_{2K})^T$, and so

$$\boldsymbol{x}^T\boldsymbol{G}_{NUM}\boldsymbol{x} = \sum_{i=1}^{K}[\beta_{1i}^2 + 2\alpha\beta_{1i}\beta_{2i} + \beta_{2i}^2]. \tag{A.7}$$

Note if $|\alpha| \leq 1$ then $\beta_{1i}^2 + 2\alpha\,\beta_{1i}\beta_{2i} + \beta_{2i}^2 \geq 0$ for all $i = 1, \ldots, K$. Hence, a sufficient condition for $\boldsymbol{x}^T\boldsymbol{G}_{NUM}\boldsymbol{x} \geq 0$ is $|\alpha| \leq 1$. So if $|\alpha| < 1$ the numerator matrix would be positive definite, and if $|\alpha| \leq 1$ the numerator matrix would be positive semi-definite.

We have shown the numerator matrix of $\boldsymbol{G}$ is positive semi-definite if $|\alpha| \leq 1$. Now consider the denominator of $\boldsymbol{G}$. The proof for the denominator matrix follows directly from Gerber et al. (2023). Define the matrix $\boldsymbol{X}$ with entries

$$x_{ij} := \frac{n_{ij}^{NN}}{T}, \tag{A.8}$$

where $n_{ij}^{NN} := |\{(i, j) : |r_{ti}| < H_i, \ |r_{tj}| < H_j\}|$. We can see $T(1 - x_{ij}) = T - n_{ij}^{NN}$ which is the denominator entry of g_{ij}. Noting that all entries $0 \leq x_{ij} < 1$ (we exclude the case

$x_{ij} = 1$ as this means $T - n_{ij}^{NN} = 0$), we can write

$$g_{ij} = \frac{\langle \boldsymbol{F}_i^{(1)}, \boldsymbol{F}_j^{(1)} \rangle + \langle \boldsymbol{F}_i^{(2)}, \boldsymbol{F}_j^{(2)} \rangle + \alpha(\langle \boldsymbol{F}_i^{(1)}, \boldsymbol{F}_j^{(2)} \rangle + \langle \boldsymbol{F}_i^{(2)}, \boldsymbol{F}_j^{(1)} \rangle)}{T(1 - x_{ij})} \tag{A.9}$$

$$= \frac{\langle \boldsymbol{F}_i^{(1)}, \boldsymbol{F}_j^{(1)} \rangle + \langle \boldsymbol{F}_i^{(2)}, \boldsymbol{F}_j^{(2)} \rangle + \alpha(\langle \boldsymbol{F}_i^{(1)}, \boldsymbol{F}_j^{(2)} \rangle + \langle \boldsymbol{F}_i^{(2)}, \boldsymbol{F}_j^{(1)} \rangle)}{T} \sum_{s=0}^{\infty} x_{ij}^s \tag{A.10}$$

using the fact that $\frac{1}{1-x_{ij}} = \sum_{s=0}^{\infty} x_{ij}^s$.

We now show that $\boldsymbol{X}$ is positive semi-definite by introducing a new matrix $\boldsymbol{P}$ with entries

$$p_{tk} := 1 - |f_{tk}^{(0)}|. \tag{A.11}$$

Then,

$$x_{ij} = \frac{n_{ij}^{NN}}{T} = \frac{\langle P_i, P_j \rangle}{T}, \tag{A.12}$$

i.e.,

$$\boldsymbol{X} = \frac{\boldsymbol{P}^T \boldsymbol{P}}{T} \tag{A.13}$$

and $\boldsymbol{X}$ is positive semi-definite as it is in the form of $\boldsymbol{Z}^T \boldsymbol{Z}$ and $1/T$ is a scalar multiplier. We can re-write g_{ij} in terms of P_i and P_j,

$$g_{ij} = \frac{\langle \boldsymbol{F}_i^{(1)}, \boldsymbol{F}_j^{(1)} \rangle + \langle \boldsymbol{F}_i^{(2)}, \boldsymbol{F}_j^{(2)} \rangle + \alpha(\langle \boldsymbol{F}_i^{(1)}, \boldsymbol{F}_j^{(2)} \rangle + \langle \boldsymbol{F}_i^{(2)}, \boldsymbol{F}_j^{(1)} \rangle)}{T} \sum_{s=0}^{\infty} \left(\frac{\langle P_i, P_j \rangle}{T} \right)^s. \tag{A.14}$$

Now we can finally re-write the correlation matrix $\boldsymbol{G}$ as

$$\boldsymbol{G} = \frac{\boldsymbol{G}_{NUM}}{T} \otimes \left(\mathbf{1} + \frac{\boldsymbol{P}^T \boldsymbol{P}}{T} + \left(\frac{\boldsymbol{P}^T \boldsymbol{P}}{T} \otimes \frac{\boldsymbol{P}^T \boldsymbol{P}}{T} \right) + \left(\frac{\boldsymbol{P}^T \boldsymbol{P}}{T} \otimes \frac{\boldsymbol{P}^T \boldsymbol{P}}{T} \otimes \frac{\boldsymbol{P}^T \boldsymbol{P}}{T} \right) + \dots \right) \tag{A.15}$$

where $\otimes$ denotes the element-wise (Hadamard) product. We can see each term in equation A.15 is positive semi-definite as $\boldsymbol{G}_{NUM}$ is positive semi-definite given $|\alpha| \leq 1$, and $\mathbf{1}$ and $\boldsymbol{P}^T \boldsymbol{P}$ are positive semi-definite. Hence, by Schur product lemma (that states that the element-wise product of positive semi-definite matrices is also a positive semi-definite matrix), $\boldsymbol{G}$ is positive semi-definite when $|\alpha| \leq 1$.

Therefore, we can also derive the 2-threshold Gerber covariance matrix $\boldsymbol{\Sigma}$ as

$$\boldsymbol{\Sigma} = \operatorname{diag}(\boldsymbol{\sigma})\,\boldsymbol{G}\,\operatorname{diag}(\boldsymbol{\sigma}) \tag{A.16}$$

where $\boldsymbol{\sigma}$ is a $K \times 1$ vector of sample standard deviations of the set of historical asset returns. This is also positive semi-definite as it is a valid covariance matrix of a set of random variables. In solving the optimization problem such as problem 1.2 as part of portfolio optimization process, the covariance matrix $\boldsymbol{\Sigma}$ is used.

A.2   3-threshold Gerber correlation

In this section we derive sufficient conditions for positive semi-definiteness of the 3-threshold Gerber correlation. We take a similar approach as in the case for 2-threshold Gerber correlation.

Define new functions of r_{tk} and thresholds C_1, C_2, C_3

$$f_{tk}^{(0)} = \begin{cases} 1 & \text{if } r_{tk} \geq C_1 \\ -1 & \text{if } r_{tk} < -C_1 \\ 0 & \text{otherwise} \end{cases} \tag{A.17}$$

$$f_{tk}^{(1)} = \begin{cases} 1 & \text{if } C_1 \leq r_{tk} < C_2 \\ -1 & \text{if } -C_2 \leq r_{tk} < -C_1 \\ 0 & \text{otherwise} \end{cases} \tag{A.18}$$

$$f_{tk}^{(2)} = \begin{cases} 1 & \text{if } C_2 \leq r_{tk} < C_3 \\ -1 & \text{if } -C_3 \leq r_{tk} < -C_2 \\ 0 & \text{otherwise} \end{cases} \tag{A.19}$$

$$f_{tk}^{(3)} = \begin{cases} 1 & \text{if } r_{tk} \geq C_3 \\ -1 & \text{if } r_{tk} < -C_3 \\ 0 & \text{otherwise.} \end{cases} \tag{A.20}$$

We can express the numerator of g_{ij} as

$$
\begin{aligned}
\sum_{i=1}^{T} m_{ij}(t) = &\langle \boldsymbol{F}_i^{(1)}, \boldsymbol{F}_j^{(1)} \rangle + \langle \boldsymbol{F}_i^{(2)}, \boldsymbol{F}_j^{(2)} \rangle + \langle \boldsymbol{F}_i^{(3)}, \boldsymbol{F}_j^{(3)} \rangle \\
&+ \alpha_2 (\langle \boldsymbol{F}_i^{(1)}, \boldsymbol{F}_j^{(2)} \rangle + \langle \boldsymbol{F}_i^{(2)}, \boldsymbol{F}_j^{(1)} \rangle + \langle \boldsymbol{F}_i^{(3)}, \boldsymbol{F}_j^{(2)} \rangle + \langle \boldsymbol{F}_i^{(2)}, \boldsymbol{F}_j^{(3)} \rangle) \\
&+ \alpha_3 (\langle \boldsymbol{F}_i^{(3)}, \boldsymbol{F}_j^{(1)} \rangle + \langle \boldsymbol{F}_i^{(1)}, \boldsymbol{F}_j^{(3)} \rangle).
\end{aligned}
\tag{A.21}
$$

We can express the numerator matrix of 3-threshold Gerber correlation matrix $\boldsymbol{G}$ with entries g_{ij} as

$$
\begin{aligned}
\boldsymbol{G}_{NUM} = &\boldsymbol{F}^{(1)T} \boldsymbol{F}^{(1)} + \boldsymbol{F}^{(2)T} \boldsymbol{F}^{(2)} + \boldsymbol{F}^{(3)T} \boldsymbol{F}^{(3)} \\
&+ \alpha_2 (\boldsymbol{F}^{(1)T} \boldsymbol{F}^{(2)} + \boldsymbol{F}^{(2)T} \boldsymbol{F}^{(1)} + \boldsymbol{F}^{(3)T} \boldsymbol{F}^{(2)} + \boldsymbol{F}^{(2)T} \boldsymbol{F}^{(3)}) \\
&+ \alpha_3 (\boldsymbol{F}^{(3)T} \boldsymbol{F}^{(1)} + \boldsymbol{F}^{(1)T} \boldsymbol{F}^{(3)}).
\end{aligned}
\tag{A.22}
$$

$\boldsymbol{G}_{NUM}$ is positive semi-definite when $\boldsymbol{x}^T \boldsymbol{G}_{NUM} \boldsymbol{x} \geq 0$ for any vector $\boldsymbol{x} \in \mathbb{R}^K$. Now,

$$
\begin{aligned}
\boldsymbol{x}^T \boldsymbol{G}_{NUM} \boldsymbol{x} = &(\boldsymbol{F}^{(1)} \boldsymbol{x})^T (\boldsymbol{F}^{(1)} \boldsymbol{x}) + (\boldsymbol{F}^{(2)} \boldsymbol{x})^T (\boldsymbol{F}^{(2)} \boldsymbol{x}) + (\boldsymbol{F}^{(3)} \boldsymbol{x})^T (\boldsymbol{F}^{(3)} \boldsymbol{x}) + \\
&+ \alpha_2 [(\boldsymbol{F}^{(1)} \boldsymbol{x})^T (\boldsymbol{F}^{(2)} \boldsymbol{x}) + (\boldsymbol{F}^{(2)} \boldsymbol{x})^T (\boldsymbol{F}^{(1)} \boldsymbol{x}) + (\boldsymbol{F}^{(3)} \boldsymbol{x})^T (\boldsymbol{F}^{(2)} \boldsymbol{x}) \\
&+ (\boldsymbol{F}^{(2)} \boldsymbol{x})^T (\boldsymbol{F}^{(3)} \boldsymbol{x})] + \alpha_3 [(\boldsymbol{F}^{(3)} \boldsymbol{x})^T (\boldsymbol{F}^{(1)} \boldsymbol{x}) + (\boldsymbol{F}^{(1)} \boldsymbol{x})^T (\boldsymbol{F}^{(3)} \boldsymbol{x})].
\end{aligned}
\tag{A.23}
$$

Denote $\boldsymbol{F}^{(s)} \boldsymbol{x} = (\beta_{s1}, \ldots, \beta_{sK})^T$, we have

$$
\boldsymbol{x}^T \boldsymbol{G}_{NUM} \boldsymbol{x} = \sum_{i=1}^{K} \left[\beta_{1i}^2 + \beta_{2i}^2 + \beta_{3i}^2 + 2\alpha_2 (\beta_{1i}\beta_{2i} + \beta_{2i}\beta_{3i}) + 2\alpha_3 \beta_{1i}\beta_{3i} \right].
\tag{A.24}
$$

We wish to find the values of α_2 and α_3 for which $\boldsymbol{x}^T \boldsymbol{G}_{NUM} \boldsymbol{x} \geq 0$. A sufficient condition is

$$
\beta_{1i}^2 + \beta_{2i}^2 + \beta_{3i}^2 + 2\alpha_2 (\beta_{1i}\beta_{2i} + \beta_{2i}\beta_{3i}) + 2\alpha_3 \beta_{1i}\beta_{3i} \geq 0,
\tag{A.25}
$$

for all $i = 1, \ldots, K$.

The trivial solution of $(\beta_{1i}, \beta_{2i}, \beta_{3i}) = (0, 0, 0)$ makes the LHS of equation A.25 equal to 0. To check for a wider region where the inequality also satisfies, we find the conditions for positive definiteness of the Hessian matrix as it will mean the LHS will attain a local minimum of value 0. We can compute the Hessian matrix as

$$\tilde{\boldsymbol{H}} = \begin{bmatrix} 2 & 2\alpha_2 & 2\alpha_3 \\ 2\alpha_2 & 2 & 2\alpha_2 \\ 2\alpha_3 & 2\alpha_2 & 2 \end{bmatrix}.$$

Let $\boldsymbol{H} = \frac{1}{2}\tilde{\boldsymbol{H}}$. We require α_2 and α_3 such that $\boldsymbol{H} \succ 0$, i.e., all principal minors of $\boldsymbol{H}$ must have non-negative determinant. These conditions are

$$\begin{cases} 1 - \alpha_2^2 > 0 \\ 1 + 2\alpha_2^2\alpha_3 - \alpha_3^2 - 2\alpha_2^2 > 0. \end{cases} \tag{A.26}$$

The first condition of equation A.26 implies $|\alpha_2| < 1$. For the second equation, we can rewrite the condition as

$$(1 - \alpha_3)(1 + \alpha_3 - 2\alpha_2^2) > 0. \tag{A.27}$$

Equation A.27 is satisfied when

$$\begin{cases} \alpha_3 < 1 \\ \alpha_3 + 1 > 2\alpha_2^2 \end{cases} \tag{A.28}$$

or

$$\begin{cases} \alpha_3 > 1 \\ \alpha_3 + 1 < 2\alpha_2^2. \end{cases} \tag{A.29}$$

It is easy to see that given the condition $|\alpha_2| < 1$, there are no feasible values of (α_2, α_3) that satisfy equation A.29. Hence we simply consider the conditions in equation A.28.

Combining, $\boldsymbol{H} \succ 0$ when

$$\begin{cases} |\alpha_2| < 1 \\ \alpha_3 < 1 \\ \alpha_3 + 1 > 2\alpha_2^2. \end{cases} \tag{A.30}$$

Above are also the sufficient conditions on positive semi-definiteness of $\boldsymbol{G}_{NUM}$.

Figure A.1 visualizes the three conditions from equation A.30 where the x- and y-axes are for α_2 and α_3, respectively. The condition $|\alpha_2| < 1$ is shown in green, $\alpha_3 \leq 1$ is shown in red, and $\alpha_3 + 1 \geq 2\alpha_2^2$ is shown in blue. The intersection of all three regions shows the feasible region of α_2 and α_3. Now that we have shown the numerator matrix of $\boldsymbol{G}_{NUM}$ is positive semi-definite under conditions of A.30, it remains to use this property to prove

FIGURE A.1: Intersection of three graphed regions shows the feasible values of α_2 (x-axis) and α_3 (y-axis) for positive semi-definiteness of numerator matrix of Gerber correlation matrix, $\boldsymbol{G}_{NUM}$.
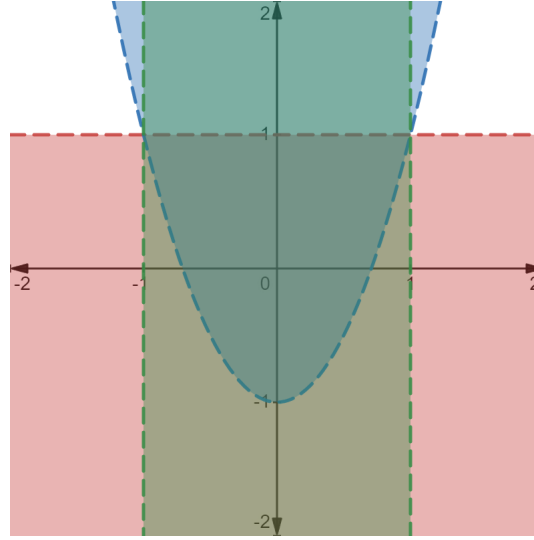
for the positive semi-definiteness of the whole 3-T Gerber correlation matrix $\boldsymbol{G}$. Define $\mathbf{X}$ with entries

$$x_{ij} := \frac{n_{ij}^{NN}}{T}, \tag{A.31}$$

where $n_{ij}^{NN} := |\{(i,j) : |r_{ti}| < C_1, \ |r_{tj}| < C_1\}|$. Rewriting g_{ij} we have

$$g_{ij} = \frac{\sum_{i=1}^{K} m_{ij}(t)}{T(1 - x_{ij})} \tag{A.32}$$

$$= \frac{\sum_{i=1}^{K} m_{ij}(t)}{T} \sum_{s=0}^{\infty} x_{ij}^{s} \tag{A.33}$$

where the numerator comes from equation A.21. Introduce $\boldsymbol{P}$ with entries $p_{tk} := 1 - |f_{tk}^{(0)}|$. Then $x_{ij} = \frac{\langle P_i, P_j \rangle}{T}$ and so $\boldsymbol{X} = \frac{\boldsymbol{P}^T \boldsymbol{P}}{T}$. This shows $\boldsymbol{X}$ is positive semi-definite.

Re-write g_{ij} in terms of P_i and P_j as

$$g_{ij} = \frac{\sum_{i=1}^{K} m_{ij}(t)}{T} \sum_{s=0}^{\infty} \left(\frac{\langle P_i, P_j \rangle}{T} \right)^{s}. \tag{A.34}$$

Finally re-write the correlation matrix $\boldsymbol{G}$ as

$$\boldsymbol{G} = \frac{\boldsymbol{G}_{NUM}}{T} \otimes \left(\mathbf{1} + \frac{\boldsymbol{P}^T \boldsymbol{P}}{T} + \left(\frac{\boldsymbol{P}^T \boldsymbol{P}}{T} \otimes \frac{\boldsymbol{P}^T \boldsymbol{P}}{T} \right) + \left(\frac{\boldsymbol{P}^T \boldsymbol{P}}{T} \otimes \frac{\boldsymbol{P}^T \boldsymbol{P}}{T} \otimes \frac{\boldsymbol{P}^T \boldsymbol{P}}{T} \right) + \dots \right). \tag{A.35}$$

By Schur product lemma, 3-threshold Gerber correlation matrix $\mathbf{G}$ is positive semi-definite, under the conditions from equation A.30.

Furthermore, equation A.35 is in the same form as the 2-threshold Gerber correlation matrix from equation A.15. The only key difference is in the definition of $\boldsymbol{G}_{NUM}$ that is derived from $m_{ij}(t)$. Thus, for any n-threshold Gerber correlation matrix with $n \geq 2$, proving positive semi-definiteness requires one to check the conditions under which numerator matrix is positive semi-definite. The whole correlation matrix is guaranteed to be positive semi-definite under such conditions if they exist, given consistent definition of n_{ij}^{NN}.

A.3 n-threshold Gerber correlation

In this section we derive sufficient conditions for positive semi-definiteness of the n-threshold Gerber correlation.

Define new functions of r_{tk} and thresholds $C_1, \ldots, C_s, \ldots, C_n$:

$$f_{tk}^{(0)} = \begin{cases} 1 & \text{if } r_{tk} \geq C_1 \\ -1 & \text{if } r_{tk} < -C_1 \\ 0 & \text{otherwise} \end{cases} \tag{A.36}$$

$$f_{tk}^{(1)} = \begin{cases} 1 & \text{if } C_1 \leq r_{tk} < C_2 \\ -1 & \text{if } -C_2 \leq r_{tk} < -C_1 \\ 0 & \text{otherwise} \end{cases} \tag{A.37}$$

$$f_{tk}^{(s)} = \begin{cases} 1 & \text{if } C_s \leq r_{tk} < C_{s+1} \\ -1 & \text{if } -C_{s+1} \leq r_{tk} < -C_s \\ 0 & \text{otherwise} \end{cases} \tag{A.38}$$

$$f_{tk}^{(n)} = \begin{cases} 1 & \text{if } r_{tk} \geq C_n \\ -1 & \text{if } r_{tk} < -C_n \\ 0 & \text{otherwise.} \end{cases} \tag{A.39}$$

We can express the numerator of g_{ij} as

$$
\begin{aligned}
\sum_{i=1}^{T} m_{ij}(t) = {} & \sum_{l=1}^{n} \langle \boldsymbol{F}_i^{(l)}, \boldsymbol{F}_j^{(l)} \rangle \\
& + \alpha_2 \sum_{l=1}^{n-1} \left[\langle \boldsymbol{F}_i^{(l)}, \boldsymbol{F}_j^{(l+1)} \rangle + \langle \boldsymbol{F}_i^{(l+1)}, \boldsymbol{F}_j^{(l)} \rangle \right] \\
& + \alpha_3 \sum_{l=1}^{n-2} \left[\langle \boldsymbol{F}_i^{(l)}, \boldsymbol{F}_j^{(l+2)} \rangle + \langle \boldsymbol{F}_i^{(l+2)}, \boldsymbol{F}_j^{(l)} \rangle \right] \\
& + \ldots \\
& + \alpha_s \sum_{l=1}^{n-s+1} \left[\langle \boldsymbol{F}_i^{(l)}, \boldsymbol{F}_j^{(l+s-1)} \rangle + \langle \boldsymbol{F}_i^{(l+s-1)}, \boldsymbol{F}_j^{(l)} \rangle \right] \\
& + \ldots \\
& + \alpha_{n-1} \sum_{l=1}^{2} \left[\langle \boldsymbol{F}_i^{(l)}, \boldsymbol{F}_j^{(l+n-2)} \rangle + \langle \boldsymbol{F}_i^{(l+n-2)}, \boldsymbol{F}_j^{(l)} \rangle \right] \\
& + \alpha_n \left[\langle \boldsymbol{F}_i^{(1)}, \boldsymbol{F}_j^{(n)} \rangle + \langle \boldsymbol{F}_i^{(n)}, \boldsymbol{F}_j^{(1)} \rangle \right].
\end{aligned}
$$

We can express the numerator matrix of n-threshold Gerber correlation matrix $\boldsymbol{G}$ with entries g_{ij} as

$$
\begin{aligned}
\boldsymbol{G}_{NUM} := {} & \sum_{l=1}^{n} \boldsymbol{F}^{(l)T} \boldsymbol{F}^{(l)} \\
& + \alpha_2 \sum_{l=1}^{n-1} \left[\boldsymbol{F}^{(l)T} \boldsymbol{F}^{(l+1)} + \boldsymbol{F}^{(l+1)T} \boldsymbol{F}^{(l)} \right] \\
& + \ldots \\
& + \alpha_{n-1} \sum_{l=1}^{2} \left[\boldsymbol{F}^{(l)T} \boldsymbol{F}^{(l+n-2)} + \boldsymbol{F}^{(l+n-2)T} \boldsymbol{F}^{(l)} \right] \\
& + \alpha_n \left[\boldsymbol{F}^{(1)T} \boldsymbol{F}^{(n)} + \boldsymbol{F}^{(n)T} \boldsymbol{F}^{(1)} \right].
\end{aligned}
$$

G_{NUM} is positive semi-definite when $\boldsymbol{x}^T\boldsymbol{G}_{NUM}\boldsymbol{x} \geq 0$ for any vector $\boldsymbol{x} \in \mathbb{R}^K$. Now,

$$\boldsymbol{x}^T\boldsymbol{G}_{NUM}\boldsymbol{x} = \sum_{l=1}^{n}(\boldsymbol{F}^{(l)}\boldsymbol{x})^T(\boldsymbol{F}^{(l)}\boldsymbol{x})$$

$$+ \alpha_2 \sum_{l=1}^{n-1}\left[(\boldsymbol{F}^{(l)}\boldsymbol{x})^T(\boldsymbol{F}^{(l+1)}\boldsymbol{x}) + (\boldsymbol{F}^{(l+1)}\boldsymbol{x})^T(\boldsymbol{F}^{(l)}\boldsymbol{x})\right]$$

$$+ \ldots$$

$$+ \alpha_n \left[(\boldsymbol{F}^{(1)}\boldsymbol{x})^T(\boldsymbol{F}^{(n)}\boldsymbol{x}) + (\boldsymbol{F}^{(n)}\boldsymbol{x})^T(\boldsymbol{F}^{(1)}\boldsymbol{x})\right].$$

Denote $\boldsymbol{F}^{(s)}\boldsymbol{x} = (\beta_{s1}, \ldots, \beta_{sK})^T$, we have

$$\boldsymbol{x}^T\boldsymbol{G}_{NUM}\boldsymbol{x} = \sum_{i=1}^{K}\left[\sum_{s=1}^{n}\beta_{si}^2 + 2\alpha_2 \sum_{s=1}^{n-1}\beta_{si}\beta_{s+1,i} + \ldots + 2\alpha_n\beta_{1i}\beta_{ni}\right]. \qquad (A.40)$$

We wish to find the values of $\alpha_2, \ldots, \alpha_n$ for which $\boldsymbol{x}^T\boldsymbol{G}_{NUM}\boldsymbol{x} \geq 0$. A sufficient condition is

$$\sum_{s=1}^{n}\beta_{si}^2 + 2\alpha_2 \sum_{s=1}^{n-1}\beta_{si}\beta_{s+1,i} + \ldots + 2\alpha_n\beta_{1i}\beta_{ni} \geq 0, \qquad (A.41)$$

for all $i = 1, \ldots, K$.

The trivial solution of $(\beta_{1i}, \ldots, \beta_{ni}) = \boldsymbol{0}$ makes the LHS of equation A.41 equal to 0. To check for a wider region where the inequality also satisfies, we find the conditions for positive definiteness of the Hessian matrix as it will mean the LHS will attain a local minimum of value 0. We can compute the Hessian matrix as $\tilde{\boldsymbol{H}}$ and define $\boldsymbol{H} := \frac{1}{2}\tilde{\boldsymbol{H}}$ which gives

$$\boldsymbol{H} = \begin{bmatrix} 1 & \alpha_2 & \alpha_3 & \alpha_4 & \cdots & \alpha_n \\ \alpha_2 & 1 & \alpha_2 & \alpha_3 & \cdots & \alpha_{n-1} \\ \alpha_3 & \alpha_2 & 1 & \alpha_2 & \cdots & \alpha_{n-2} \\ \alpha_4 & \alpha_3 & \alpha_2 & 1 & \cdots & \alpha_{n-3} \\ \vdots & \vdots & \vdots & \vdots & \ddots & \vdots \\ \alpha_n & \alpha_{n-1} & \alpha_{n-2} & \alpha_{n-3} & \cdots & 1 \end{bmatrix}.$$

To find a simple but crude sufficient condition for $\boldsymbol{H}$ to be positive semi-definite we decompose $\boldsymbol{H}$ into a sum of $n-1$ symmetric matrices as

$$\boldsymbol{H} = \begin{bmatrix} u_2 & \alpha_2 & 0 & 0 & \cdots & 0 \\ \alpha_2 & u_2 & \alpha_2 & 0 & \cdots & 0 \\ 0 & \alpha_2 & u_2 & \alpha_2 & \cdots & 0 \\ 0 & 0 & \alpha_2 & u_2 & \cdots & 0 \\ \vdots & \vdots & \vdots & \vdots & \ddots & \vdots \\ 0 & 0 & 0 & 0 & \cdots & u_2 \end{bmatrix} + \begin{bmatrix} u_3 & 0 & \alpha_3 & 0 & \cdots & 0 \\ 0 & u_3 & 0 & \alpha_3 & \cdots & 0 \\ \alpha_3 & 0 & u_3 & 0 & \cdots & 0 \\ 0 & \alpha_3 & 0 & u_3 & \cdots & 0 \\ \vdots & \vdots & \vdots & \vdots & \ddots & \vdots \\ 0 & 0 & 0 & 0 & \cdots & u_3 \end{bmatrix} + \ldots$$

$$+ \begin{bmatrix} u_n & 0 & 0 & 0 & \cdots & \alpha_n \\ 0 & u_n & 0 & 0 & \cdots & 0 \\ 0 & 0 & u_n & 0 & \cdots & 0 \\ 0 & 0 & 0 & u_n & \cdots & 0 \\ \vdots & \vdots & \vdots & \vdots & \ddots & \vdots \\ \alpha_n & 0 & 0 & 0 & \cdots & u_n \end{bmatrix}$$

$$=: \boldsymbol{H}_2 + \boldsymbol{H}_3 + \ldots + \boldsymbol{H}_n.$$

where $\sum_{i=2}^{n} u_i = 1$ with $u_i \geq 0 \ \forall \ i$. We note that for $\boldsymbol{H}_i$ where $i = 2, \ldots \lceil \frac{n}{2} \rceil$ there are two α_i's in each row, and for $\boldsymbol{H}_i$ where $i = \lceil \frac{n}{2} \rceil + 1, \ldots, n$ there is only one α_i in each row.

A sufficient condition for $\boldsymbol{H} \succ 0$ is at least one of the decomposed matrix $\boldsymbol{H}_i$ being positive definite and the rest positive semi-definite. For this we use the property of diagonally dominant matrices. A square matrix is said to be diagonally dominant if, for every row of the matrix, the magnitude of the diagonal entry in a row is larger than or equal to the sum of the magnitudes of all the other non-diagonal entries in that row, i.e.,

$$|u_{ii}| \geq \sum_{i \neq j} |u_{ij}| \quad \text{for all } i. \tag{A.42}$$

The matrix is called strictly diagonally dominant if a strict inequality is satisfied. Key property is that a symmetric, strictly diagonally dominant matrix with positive diagonal entries is positive definite. Similarly, a symmetric, diagonally dominant matrix with non-negative diagonal entries is positive semi-definite.

Hence, a sufficient condition for $\boldsymbol{H} \succ 0$ translates to at least one of the decomposed matrices being strictly diagonally dominant and others being diagonally dominant.

From the decomposed matrices, we find $\boldsymbol{H}_i$ is diagonally dominant when

$$\alpha_i \leq \begin{cases} \frac{u_i}{2} & \text{if } i = 2, \ldots, \lceil \frac{n}{2} \rceil \\ u_i & \text{if } i = \lceil \frac{n}{2} \rceil + 1, \ldots, n \end{cases} \tag{A.43}$$

and strictly diagonally dominant for any $\boldsymbol{H}_i$ if a strict inequality is used.

For simplicity we weaken the condition on α_i for $i = \lceil \frac{n}{2} \rceil + 1, \ldots, n$ to $\frac{u_i}{2}$ and have for all $i = 2, \ldots, n$

$$\alpha_i \leq \frac{u_i}{2}. \tag{A.44}$$

As $\sum_{i=2}^{n} u_i = 1$ we have

$$\sum_{i=2}^{n} \alpha_i \leq \sum_{i=2}^{n} \frac{u_i}{2}$$
$$= \frac{1}{2}.$$

Therefore, the condition $\sum_{i=2}^{n} \alpha_i \leq \frac{1}{2}$ is a sufficient condition for all $\boldsymbol{H}_i$'s being positive semi-definite. For $\boldsymbol{H}$ to be positive definite, we also need at least one $\boldsymbol{H}_i$ being positive definite (strictly diagonally dominant). This means at least one $\boldsymbol{H}_i$ needs to satisfy the condition A.42 with a strict inequality and with positive diagonal entries. This translates to the condition

$$\sum_{i=2}^{n} \alpha_i < \frac{1}{2} \text{ and at least one } \alpha_i > 0. \tag{A.45}$$

Above is a sufficient condition for the Hessian matrix $\boldsymbol{H}$ to be positive definite, and hence $\boldsymbol{x}^T \boldsymbol{G}_{NUM} \boldsymbol{x}$ to be positive semi-definite.

From A.2 we saw positive semi-definiteness of Gerber correlation matrix depends only on the positive semi-definiteness of the numerator matrix $\boldsymbol{x}^T \boldsymbol{G}_{NUM} \boldsymbol{x}$. Thus, a simple but crude sufficient condition for positive semi-definiteness of n-threshold Gerber correlation matrix with $n \geq 2$ is $\sum_{i=2}^{n} \alpha_i < \frac{1}{2}$ with at least one i such that $0 < \alpha_i < \frac{u_i}{2}$.

It can be noted that the sufficient condition A.45 is quite a strict one. For example, for 3-threshold Gerber correlation, feasible values of α_2 and α_3 obtained from the condition

A.45 are a subset of feasible values from the condition A.30. Figure A.2 illustrates this graphically.

FIGURE A.2: **Red**: Feasible values of α_2 (x-axis) and α_3 (y-axis) for positive semi-definiteness (excluding the origin) from the sufficient condition of n-threshold Gerber correlation in A.45. **Green**: Feasible values from the sufficient condition of 3-threshold Gerber correlation in A.30.
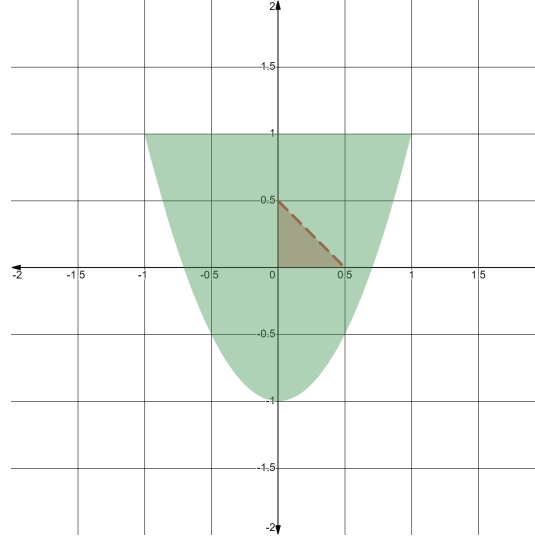
Appendix B

Appendix for Simulation Study

TABLE B.1: Simulation results showing number of repetitions with positive semi-definite correlation matrices for 3-threshold Gerber correlation as defined in (2.8). Common thresholds of $C_1 = 0.5, C_2 = 1, C_3 = 1.5$ used for all assets $k = 1, \ldots, K$.

	$(\alpha_1, \alpha_2, \alpha_3)$	Satisfies 2.7	Positive semi-definite matrices
0	(1, 0.0, 0.0)	True	1000
1	(1, 0.0, -0.5)	True	1000
2	(1, -0.5, 0.0)	True	1000
3	(1, -0.5, 0.5)	True	1000
4	(1, 0.0, 0.5)	True	1000
5	(1, 0.5, 0.5)	True	1000
6	(1, 0.5, 0.0)	True	1000
7	(1, -1.5, 1.5)	False	1000
8	(1, -1.0, 1.5)	False	1000
9	(1, 1.5, 0.0)	False	1000
10	(1, 1.0, 1.5)	False	1000
11	(1, -1.5, 0.5)	False	762
12	(1, -1.0, 0.5)	False	1000
13	(1, 0.5, 1.5)	False	1000
14	(1, 0.0, 1.5)	False	1000
15	(1, -0.5, 1.5)	False	1000
16	(1, 1.0, 0.5)	False	1000
17	(1, 1.5, 1.0)	False	1000
18	(1, 1.5, 0.5)	False	1000
19	(1, -1.5, 1.0)	False	1000
20	(1, 1.0, 0.0)	False	1000
21	(1, -0.5, 1.0)	False	1000
22	(1, 0.0, 1.0)	False	1000
23	(1, 0.5, 1.0)	False	1000
24	(1, 1.0, 1.0)	False	1000
25	(1, -1.0, 1.0)	False	1000
26	(1, -1.5, -1.5)	False	0
27	(1, -1.0, -1.5)	False	0
28	(1, -1.0, 0.0)	False	1000
29	(1, -0.5, -1.5)	False	1000
30	(1, 0.0, -1.5)	False	1000
31	(1, 0.5, -1.5)	False	1000
32	(1, 1.0, -1.5)	False	1000
33	(1, 1.5, -1.5)	False	1000
34	(1, -1.5, -1.0)	False	0
35	(1, -1.0, -1.0)	False	10
36	(1, -0.5, -1.0)	False	1000
37	(1, 0.0, -1.0)	False	1000
38	(1, 0.5, -1.0)	False	1000
39	(1, 1.0, -1.0)	False	1000
40	(1, 1.5, -1.0)	False	1000
41	(1, -1.5, -0.5)	False	0
42	(1, -1.0, -0.5)	False	1000
43	(1, -0.5, -0.5)	False	1000
44	(1, 0.5, -0.5)	False	1000
45	(1, 1.0, -0.5)	False	1000
46	(1, 1.5, -0.5)	False	1000
47	(1, -1.5, 0.0)	False	2
48	(1, 1.5, 1.5)	False	1000

TABLE B.2: Simulation results showing number of repetitions with positive semi-definite correlation matrices for tanh-tanh Gerber correlation as defined in (3.5). For each (a, b, c, d) simulation was repeated 100 times.

	(a, b, c, d)	Positive semi-definite matrices
0	(1, 1, 0, 0)	0
1	(1, 1, -0.5, 0)	31
2	(1, 1, 0.5, 0)	44
3	(1, 1, 0, -0.5)	27
4	(1, 1, 0, 0.5)	36
5	(1, 2, 0, 0)	15
6	(1, 0.5, 0, 0)	0
7	(2, 1, 0, 0)	20
8	(0.5, 1, 0, 0)	0

Appendix C

Appendix for Empirical Study

TABLE C.1: List of 22 stocks from S&P500 used for section 4.2

	Ticker	Name	Sector
1	GOOG	Alphabet Inc. (Class C)	Communication Services
2	TMUS	T-Mobile US	Communication Services
3	TPR	Tapestry, Inc.	Consumer Discretionary
4	VFC	VF Corporation	Consumer Discretionary
5	K	Kellogg's	Consumer Staples
6	SYY	Sysco	Consumer Staples
7	CVX	Chevron Corporation	Energy
8	SLB	Schlumberger	Energy
9	CMA	Comerica	Financials
10	IVZ	Invesco	Financials
11	DXCM	Dexcom	Health Care
12	MCK	McKesson	Health Care
13	FAST	Fastenal	Industrials
14	FDX	FedEx	Industrials
15	KLAC	KLA Corporation	Information Technology
16	NOW	ServiceNow	Information Technology
17	ECL	Ecolab	Materials
18	WRK	WestRock	Materials
19	EXR	Extra Space Storage	Real Estate
20	WY	Weyerhaeuser	Real Estate
21	DTE	DTE Energy	Utilities
22	XEL	Xcel Energy	Utilities

FIGURE C.1: Cumulative portfolio return plots for varying target variance (across columns when plot is upright) and lookback periods L of 6, 9 and 12 months (across rows). **Green:** Returns using 2-threshold Gerber covariance matrix. **Orange:** 1-threshold Gerber covariance matrix returns. **Blue:** Historical covariance matrix returns.
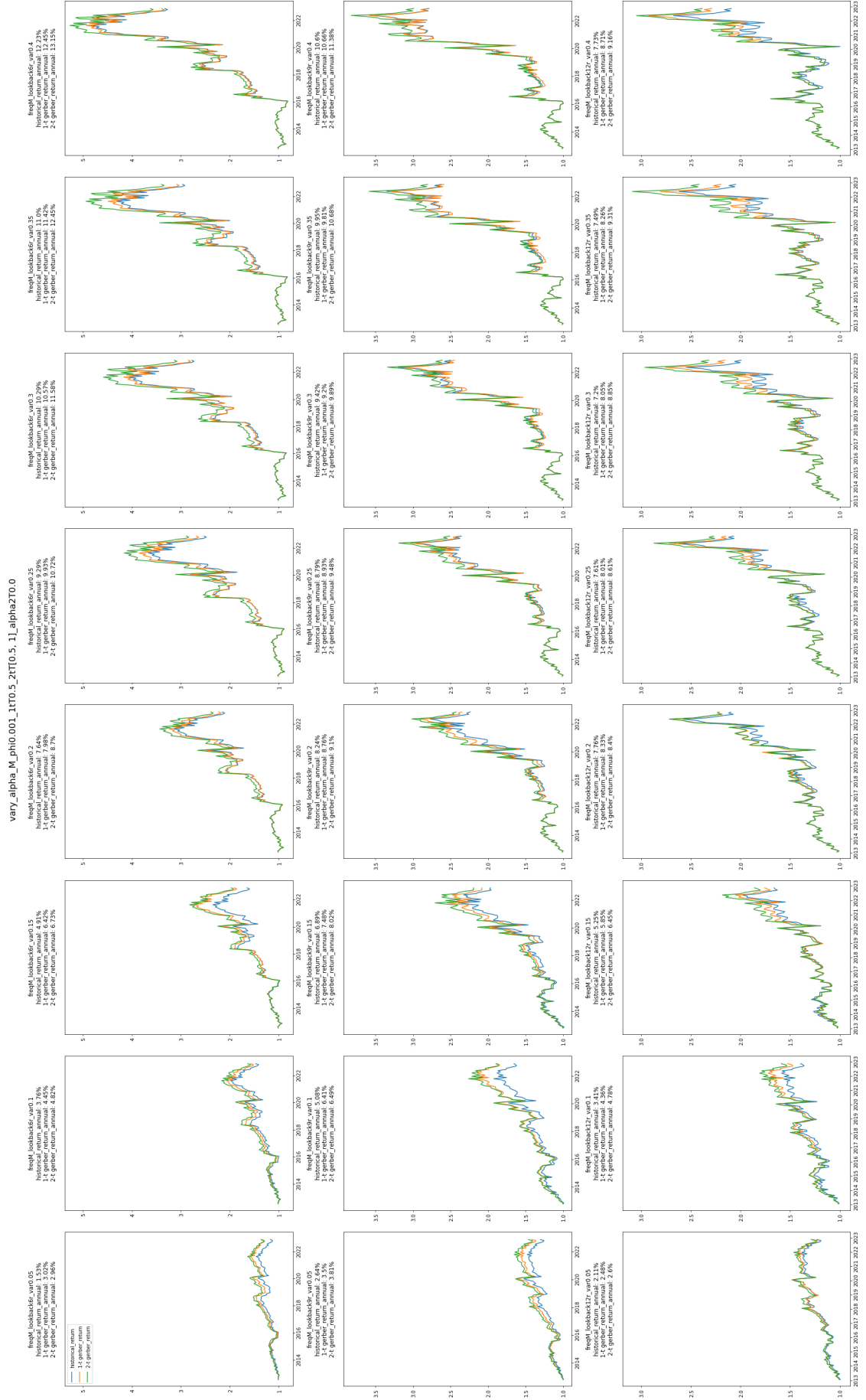
FIGURE C.2: Box plot of annualized portfolio returns (for 22-asset universe) against target annualized portfolio variance obtained with varying lookback periods, grouped by α values.
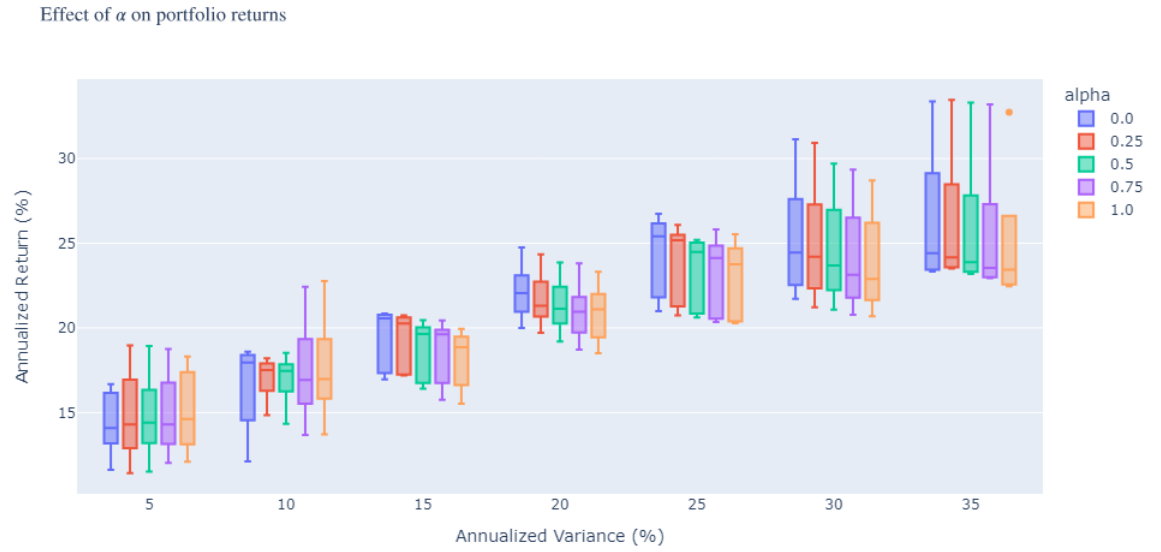

FIGURE C.3: Box plot of annualized portfolio returns (for 22-asset universe) against target annualized portfolio variance obtained with varying lookback periods, grouped by (P, Q) values.
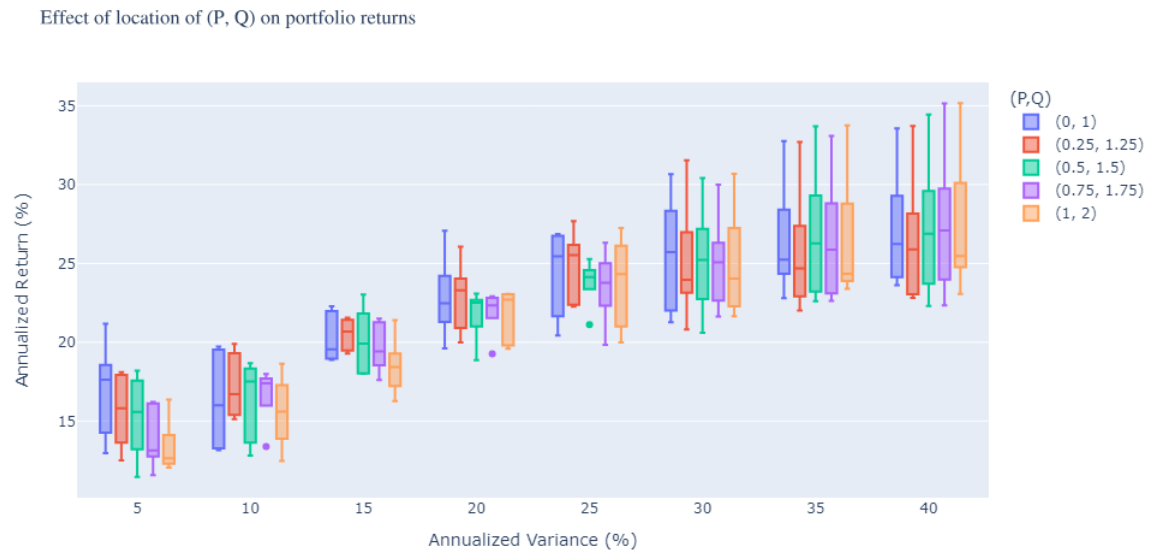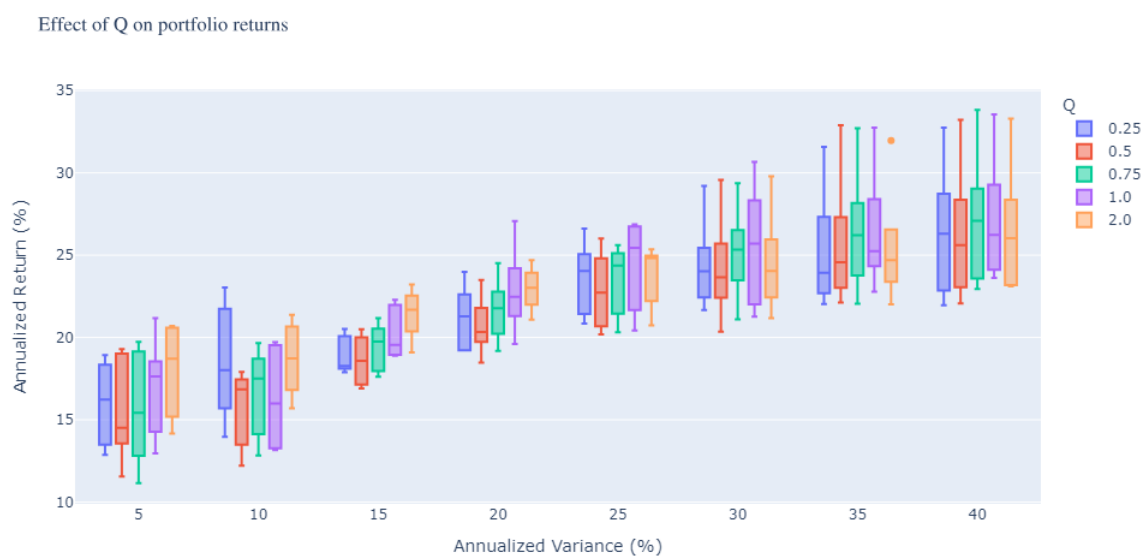
FIGURE C.4: Box plot of annualized portfolio returns (for 22-asset universe) against target annualized portfolio variance obtained with varying lookback periods, grouped by Q values.

Effect of Q on portfolio returns

Appendix D

Appendix for EWMA Gerber correlation

D.1 Positive semi-definiteness

In this section we prove that the n-threshold EWMA Gerber correlation matrix introduced in section 5.2 is positive semi-definite, as long as the underlying n-threshold Gerber correlation matrix is positive semi-definite. We work with the assumption that the ramp-up period R ensures $\sum_{s=1}^{R}\left[1 - n_{ij}^{NN}(s)\right] \neq 0$.

In equation 5.6 for $t = R$, $\hat{\boldsymbol{G}}(t)$ consists of entries $\hat{g}_{ij} = \frac{\sum_{s=1}^{R} m_{ij}(s)}{\sum_{s=1}^{R}\left[1 - n_{ij}^{NN}(s)\right]}$. This is exactly a n-threshold Gerber correlation matrix with historical time-stamps $t = 1, \ldots, R$. Hence $\hat{\boldsymbol{G}}(R)$ is positive semi-definite given that the choice of n makes the underlying n-threshold Gerber correlation matrix positive semi-definite (under suitable conditions as proven for 2- and 3-thresholds).

For $t = R+1$, we have $\hat{\boldsymbol{G}}(t-1) = \hat{\boldsymbol{G}}(R)$ being positive semi-definite, and $(1-\lambda)\hat{\boldsymbol{G}}(R)$ also being positive semi-definite as scalar multiplication preserves positive semi-definiteness.

For any $t > R$, $\tilde{\boldsymbol{G}}(t)$ is positive semi-definite, under the conditions for which the underlying n-threshold Gerber correlation matrix is positive semi-definite, since the two conditions in 5.5 reduce to standard n-threshold Gerber correlation matrix with historical time-stamp(s) t or $t - q_t, \ldots, t$. This makes $\lambda\tilde{\boldsymbol{G}}(t)$ positive semi-definite under appropriate conditions also.

Finally, we have that for $t = R$, $\hat{\boldsymbol{G}}(t)$ is positive semi-definite and also for $t = R + 1$. Assume $\hat{\boldsymbol{G}}(t)$ is positive semi-definite (under appropriate conditions where necessary) for $t = n > R + 1$, then we wish to prove $\hat{\boldsymbol{G}}(t)$ is positive semi-definite for $t = n + 1$ by mathematical induction.

We have $\hat{\boldsymbol{G}}(n+1) = \lambda \tilde{\boldsymbol{G}}(n+1) + (1-\lambda)\hat{\boldsymbol{G}}(n)$, where $\tilde{\boldsymbol{G}}(n+1)$ is positive semi-definite as we showed $\tilde{\boldsymbol{G}}(t)$ is positive semi-definite for any t. Also, we assumed $\hat{\boldsymbol{G}}(n)$ is positive semi-definite. Thus, $\hat{\boldsymbol{G}}(n+1)$ is positive semi-definite as the sum of two positive semi-definite matrices is still positive semi-definite.

Hence, by mathematical induction, we have proven that $\hat{\boldsymbol{G}}(t)$ is positive semi-definite for all $t > R$.

So, all terms in equation 5.6 are positive semi-definite under the condition for which the underlying n-threshold Gerber correlation matrix is positive semi-definite.

D.2 Empirical Study

FIGURE D.1: Box plot of annualized portfolio returns (for the 9-asset universe) against target annualized portfolio variance obtained with varying lookback periods, grouped by λ values.
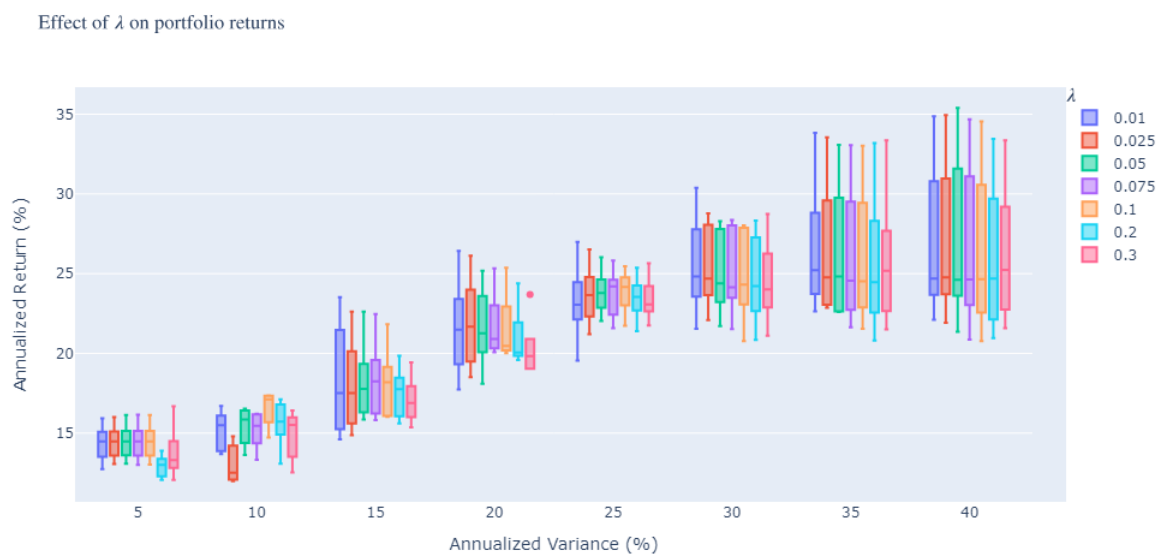
FIGURE D.2: Box plot of annualized portfolio returns (for the 22-asset universe) against target annualized portfolio variance obtained with varying lookback periods, grouped by λ values.
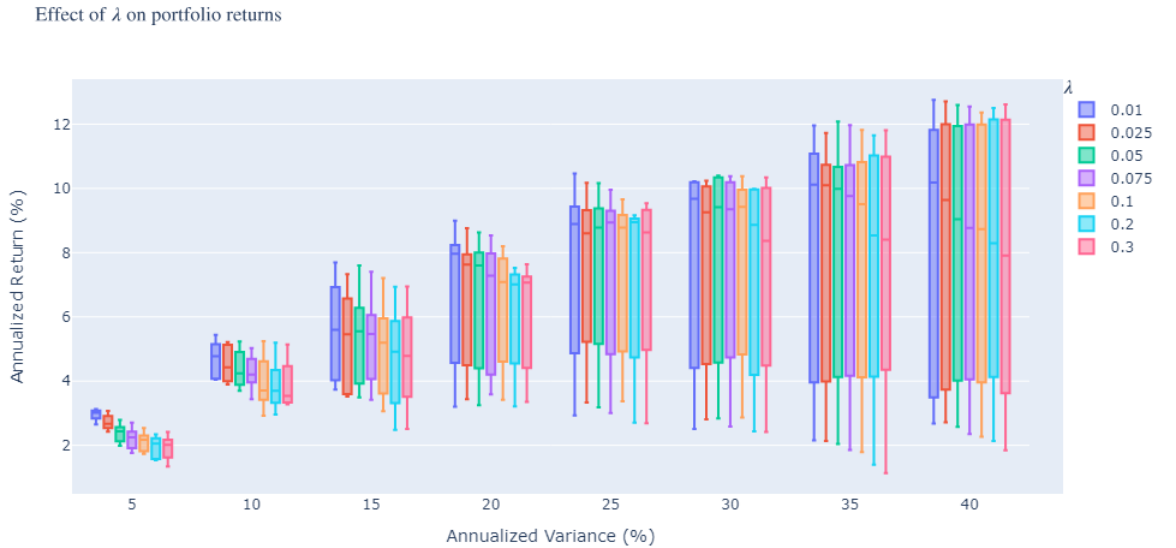
FIGURE D.3: Backtest performances on the 22-asset universe, with varying lookback periods L for fixed decay parameter $\lambda = 0.05$. **Orange:** Performance of 1-threshold EWMA Gerber covariance based portfolios. **Blue:** Performance of 1-threshold Gerber covariance based portfolios.
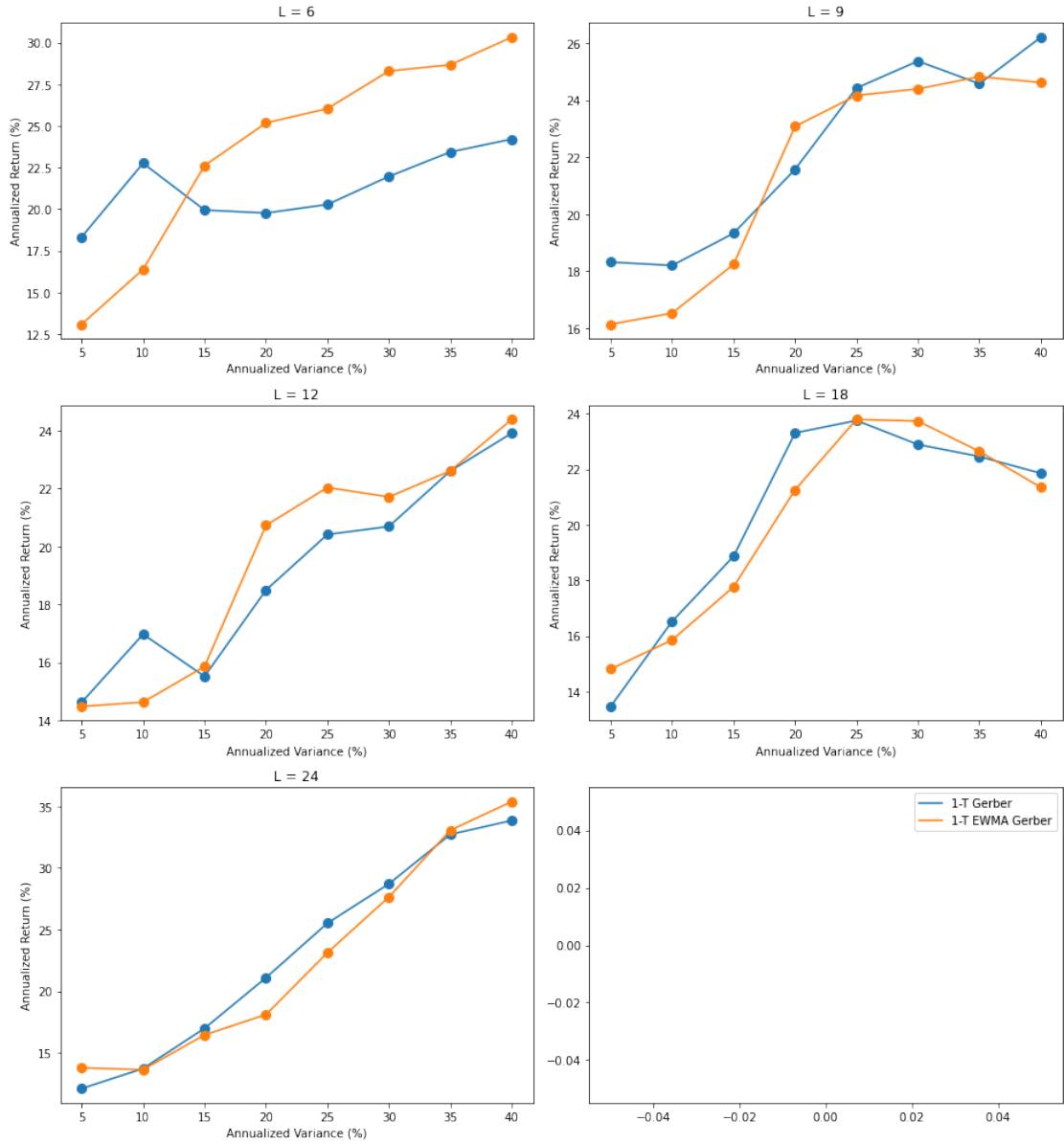
FIGURE D.4: Backtest performances on the 9-asset universe, with varying lookback periods L for fixed decay parameter $\lambda = 0.01$. **Orange:** Performance of 2-threshold EWMA Gerber covariance based portfolios. **Blue:** Performance of 2-threshold Gerber covariance based portfolios.

FIGURE D.5: Backtest performances on the 22-asset universe, with varying lookback periods L for fixed decay parameter $\lambda = 0.05$. **Orange:** Performance of 2-threshold EWMA Gerber covariance based portfolios. **Blue:** Performance of 2-threshold Gerber covariance based portfolios.
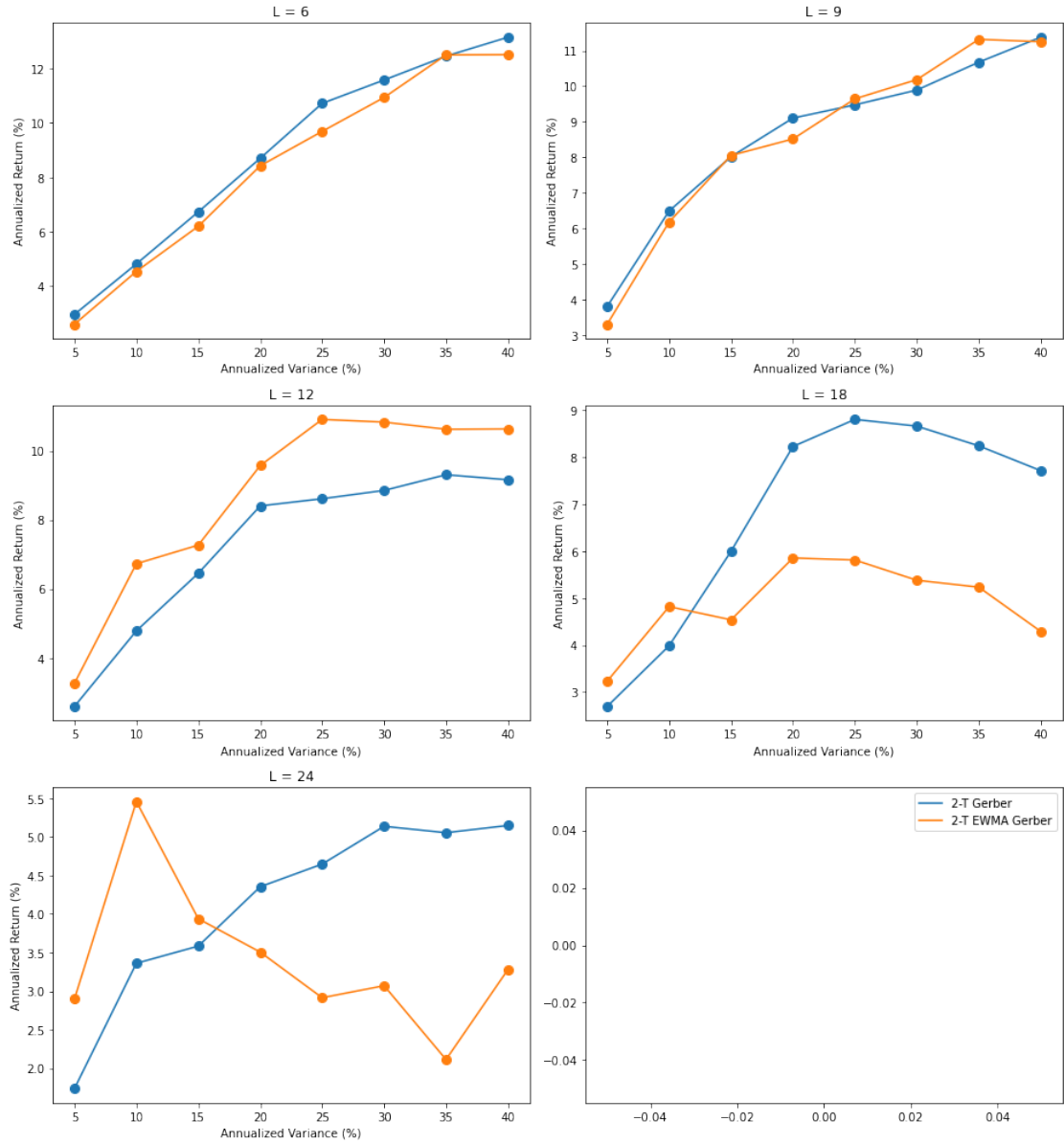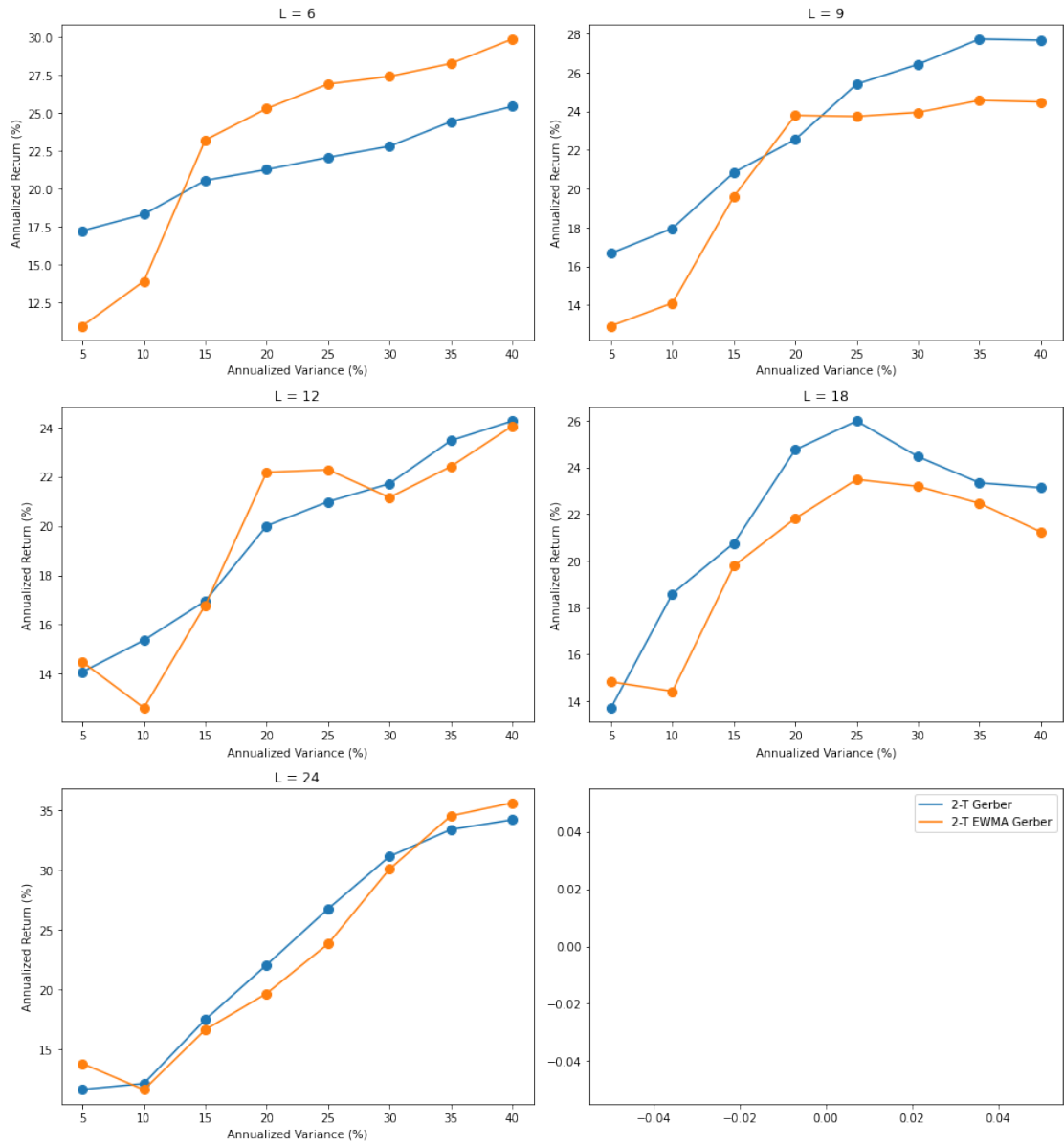
Appendix E

Appendix for Code

Python code for backtesting can be found in my github repository n-threshold-Gerber-correlation.

Bibliography

Rakesh Aggarwal and Priya Ranganathan. Common pitfalls in statistical analysis: The use of correlation techniques. *Perspectives in Clinical Research*, 4:187–190, 2016.

Alan Agresti. *Analysis of Ordinal Categorical Data*. John Wiley & Sons, 2010.

Sander Gerber, Harry M. Markowitz, Philip A. Ernst, Yinsen Miao, Babak Javid, and Paul Sargen. The gerber statistic: A robust co-movement measure for portfolio optimization. *The Journal of Portfolio Management*, 48(3):87–102, 2022. doi: http://doi.org/10.3905/jpm.2021.1.316. URL https://www.pm-research.com/content/iijpormgmt/48/3/87.

Sander Gerber, Harvey Markowitz, Pollmann Ernst, Yu Miao, Babak Javid, and Paul Sargen. Proofs that the gerber statistic is positive semidefinite. 2023. URL https://api.semanticscholar.org/CorpusID:258564256.

J. Stuart Hunter. The exponentially weighted moving average. *Journal of Quality Technology*, 18(4):203–210, 1986. doi: 10.1080/00224065.1986.11979014. URL https://doi.org/10.1080/00224065.1986.11979014.

M. G. Kendall. A NEW MEASURE OF RANK CORRELATION. *Biometrika*, 30(1-2):81–93, 06 1938. ISSN 0006-3444. doi: 10.1093/biomet/30.1-2.81. URL https://doi.org/10.1093/biomet/30.1-2.81.

Aleš Kresta. Application of garch-copula model in portfolio optimization. *Financial Assets and Investing*, 6, 2015. doi: https://doi.org/10.5817/FAI2015-2-1. URL https://journals.muni.cz/fai/article/view/7863.

Olivier Ledoit and Michael Wolf. Honey, i shrunk the sample covariance matrix. *The Journal of Portfolio Management*, 30:110–119, 2004.

Harry Markowitz. Portfolio selection*. *The Journal of Finance*, 7(1):77–91, 1952. doi: https://doi.org/10.1111/j.1540-6261.1952.tb01525.x. URL https://onlinelibrary.wiley.com/doi/abs/10.1111/j.1540-6261.1952.tb01525.x.

Roger B. Nelsen. *An Introduction to Copulas.* Springer, 2006.

Sanjiban Sekhar Roy, Rohan Chopra, Kun Chang Lee, Concetto Spampinato, and Behnam Mohammadi-ivatlood. Random forest, gradient boosted machines and deep neural network for stock price forecasting: a comparative analysis on south korean companies. *International Journal of Ad Hoc and Ubiquitous Computing*, 33(1):62–71, 2020. doi: 10.1504/IJAHUC.2020.104715. URL https://www.inderscienceonline.com/doi/abs/10.1504/IJAHUC.2020.104715.

Maziar Sahamkhadam, Andreas Stephan, and Ralf Östermark. Portfolio optimization based on garch-evt-copula forecasting models. *International Journal of Forecasting*, 34(3):497–506, 2018. ISSN 0169-2070. doi: https://doi.org/10.1016/j.ijforecast.2018.02.004. URL https://www.sciencedirect.com/science/article/pii/S0169207018300396.

Anita Yadav, C K Jha, and Aditi Sharan. Optimizing lstm for time series prediction in indian stock market. *Procedia Computer Science*, 167:2091–2100, 2020. ISSN 1877-0509. doi: https://doi.org/10.1016/j.procs.2020.03.257. URL https://www.sciencedirect.com/science/article/pii/S1877050920307237. International Conference on Computational Intelligence and Data Science.